

# Pressure in the Landau-Ginzburg Functional: Pascal's Law, Nucleation in Fluid Mixtures, a Meanfield Theory of Amphiphilic Action, and Interface Wetting in Glassy Liquids

Ho Yin Chan<sup>1</sup> and Vassiliy Lubchenko<sup>2,1,\*</sup>

<sup>1</sup>*Department of Physics, University of Houston, Houston, TX 77204-5005*

<sup>2</sup>*Department of Chemistry, University of Houston, Houston, TX 77204-5003*

(Dated: December 7, 2015)

We set up the problem of finding the transition state for phase nucleation in multi-component fluid mixtures, within the Landau-Ginzburg density functional. We establish an expression for the coordinate-dependent local pressure that applies to mixtures, arbitrary geometries, and certain non-equilibrium configurations. The expression allows one to explicitly evaluate the pressure in spherical geometry, à la van der Waals. Pascal's law is recovered within the Landau-Ginzburg density functional theory, formally analogously to how conservation of energy is recovered in the Lagrangian formulation of mechanics. We establish proper boundary conditions for certain singular functional forms of the bulk free energy density that allow one to obtain droplet solutions with thick walls in essentially closed form. The hydrodynamic modes responsible for mixing near the interface are explicitly identified in the treatment; the composition at the interface is found to depend only weakly on the droplet size. Next we develop a Landau-Ginzburg treatment of the effects of amphiphiles on the surface tension; the amphiphilic action is seen as a violation of Pascal's law. We explicitly obtain the binding potential for the detergent at the interface and the dependence of the down-renormalization of the surface tension on the activity of the detergent. Finally, we argue that the renormalization of the activation barrier for escape from long-lived structures in glassy liquids can be viewed as an action of uniformly seeded, randomly oriented amphiphilic molecules on the interface separating two dissimilar aperiodic structures. This renormalization is also considered as a "wetting" of the interface. The resulting conclusions are consistent with the random first order transition (RFOT) theory.

## I. MOTIVATION

The Gibbs phase rule<sup>1,2</sup> epitomizes the basic notion that in equilibrium, the state of a macroscopic substance is fully specified by a small set of intensive variables, such as temperature, pressure, and the molar fractions of chemically distinct components. As appreciated by Gibbs some 140 years ago, equilibria with respect to particle and momentum exchange differ from each other in a basic way: To ensure equilibrium with regard to particle exchange between distinct phases, the chemical potentials for each individual component in a mixture must be matched between the phases. In contrast, mechanical equilibrium is guaranteed already by uniformity of the full pressure; there is no need to match the *partial* pressures of individual species. Thus with each additional component in the mixture, the number of independent variables that could be in principle used to describe an equilibrium phase increases. Viewed alternatively, this means that the number of distinct phases that could be in mutual equilibrium grows with each additional component.

Situations in which some of the phases are only *finite* in size, but still containing a substantial number of molecules, can be also described rather parsimoniously with the help of equilibrium thermodynamics, at the modest expense of introducing a free energy cost of an interface between distinct phases. In this picture, the chemical potentials are still spatially uniform, while the pressure changes discontinuously across the interface, the

discontinuity scaling with the interface curvature according to the venerable Laplace formula. The corresponding limit of an infinitely-thin interface can be formulated in an internally-consistent fashion for large inclusions of minority phases,<sup>3</sup> but becomes ambiguous on molecular lengthscales because at its face value, a discontinuous pressure jump implies there is an uncompensated force acting on a subset of molecules.

In his seminal work,<sup>4,5</sup> van der Waals sought to remove this ambiguity by explicitly accounting for the free energy cost of *gradual* density variations. Within a semi-phenomenological framework equivalent to the Landau-Ginzburg functional theory but predating it by a half-century or so, van der Waals treats distinct phases in physical contact and their mutual interface on the same footing. He shows that the pressure and density change continuously across a finite-curvature interface between two coexisting phases. Van der Waals's results were rediscovered and generalized in later analyses by Cahn and Hilliard,<sup>6-8</sup> and Hart.<sup>9</sup> An alternative, quite fruitful line of work, in which the surface tension could be directly related to detailed molecular interactions, was spurred by pioneering work of Kirkwood and Buff,<sup>10</sup> see reviews in Refs. 3, 11, and 12.

Here we extend the van der Waals analysis to multi-component fluids while explicitly allowing for a density dependence of the free energy cost for spatial variations in the density itself; the latter cost generally varies between phases. Importantly, we are also able to include in the treatment situations that are steady-state only lo-

cally; this is useful for deviations from equilibrium and in the presence of chemical reactions. The present work is partially motivated by a challenging problem of current interest, viz., the formation mechanism of the puzzling mesoscopic clusters of a dense protein fluid found in some protein solutions.<sup>13–16</sup> Pan et al.<sup>16</sup> have put forth a microscopic scenario, by which the mesoscopic clusters consist of a spatially inhomogeneous, off-equilibrium mixture of monomeric protein and a transient, protein-containing complex. Already in their preliminary analysis, Pan et al.<sup>16</sup> suggest that in the presence of protein-complex formation and decay, the chemical potentials of the species involved become spatially inhomogeneous even in steady state. The inhomogeneity is largely contained within the interface and would not be captured within the thin interface approximation, thus necessitating a treatment at least at the van der Waals level. The reaction-diffusion equations are non-linear and prone to numerical instabilities; numerical solutions lack transparency that can be afforded by analytical treatment. Yet a certain class of functional forms for the bulk free energy, i.e., a collection of intersecting paraboloids, allows for analytical treatment while preserving several essential features of thick interfaces. Hereby, the free energy surface is quadratic throughout except at some well-defined dividing surface. Thus, by construction, the free energy can experience a discontinuity in the gradient and even in the function itself. How does one “patch” together the solutions for the pure phases in the presence of such singularities?

This question can be answered at the Landau-Ginzburg (LG) level, since the latter affords one a simple expression for the local pressure, which further simplifies in spherical geometry. The present treatment of local pressure is based on a formal analogy between the Landau-Ginzburg free energy functional and the mechanical action; the spatial coordinate traversing the phase boundary in the former context is analogous to the time in the latter context. In the case of macroscopic coexistence, an LG-based treatment automatically yields the familiar Pascal’s law, which is formally analogous to energy conservation in mechanics. For spherical droplets, on the other hand, there is a pressure excess inside; this excess is well approximated by the Laplace expression when the droplet is sufficiently large. We will observe that the boundary conditions that must be imposed on the order parameter at the singularity of the bulk free energy amount to a continuity of local pressure and, in fact, hearken back to conditions for macroscopic phase equilibrium elucidated by Gibbs, except that now pressure may be explicitly coordinate-dependent. The resulting treatment allows one to explicitly build the free energy profile for droplet nucleation as a function of the droplet radius and the chemical composition at the phase boundary. We establish that the composition at the droplet boundary changes little during nucleation.

The developed formalism is next generalized to situations where the local pressure is *not* spatially homogeneous even for flat interfaces. Important examples of

such situations are phase boundaries pinned by an external potential; the situation can alternatively be thought of as amphiphilic molecules collecting at phase boundaries. In the resulting, simple treatment, we explicitly observe the effects of the amphiphiles’ activity on the renormalization of the surface tension. We obtain explicit coordinate dependences of pressure and chemical potential *within* the interface, as well as the explicit form of the binding potential between the interface and the detergent. The mathematical simplicity of the formalism allows one to work both in equilibrium and away from equilibrium, in a steady-state approximation for individual phases.

The above developments turn out to afford one an arguably simplified perspective at yet another, deep problem that has been a subject of much interest and controversy,<sup>17,18</sup> namely the mechanism of activated transport in glassy liquids.<sup>19</sup> We will observe that the down-renormalization of the free energy barrier for activated transport in glassy liquids can be thought of as a decrease in the surface tension of an inter-phase boundary in the presence of uniformly seeded, randomly oriented amphiphiles. The square-root scaling of the mismatch penalty between dissimilar aperiodic structures with the size of the reconfiguring region can be viewed as a consequence of the law of large numbers. Likewise, the present formalism allows one to flesh out the “wetting” view of the mismatch penalty, due to Xia and Wolynes.<sup>20</sup> Connections with other existing treatments of glassy dynamics can be also made.

The article is organized as follows: In Section II we provide a brief pedagogical review of how to set up the problem of phase coexistence at the Landau-Ginzburg level. In Section III, we derive an expression for local pressure for the LG functional, which yields an explicit formula for spherical geometries. There we establish Pascal’s law and develop a systematic treatment of local pressure that can be applied to mixtures and off-equilibrium configurations. These results are used to obtain explicit droplet solutions for liquid mixtures in Section IV and the problem of a flat interface exposed to a pinning potential and/or amphiphilic adsorbents in Section V. These developments provide two alternative perspectives on the problem of renormalization of the mismatch penalty between dissimilar aperiodic structures in glassy liquids, which is discussed in Section VI. The final Section VII briefly summarizes the present findings.

## II. PHASE EQUILIBRIUM AND PHASE ORDERING AT LANDAU-GINZBURG LEVEL: SETUP OF THE PROBLEM

Consider a Landau-Ginzburg free energy functional:

$$F(\{\psi(\mathbf{r})\}) = \int d^3\mathbf{r} \left[ \frac{\kappa}{2} (\nabla\psi)^2 + \mathcal{V}(\psi) \right] \equiv \int d^3\mathbf{r} f(\mathbf{r}), \quad (1)$$

where  $f(\mathbf{r}) \equiv \kappa(\nabla\psi)^2/2 + \mathcal{V}(\psi)$  is thus the local free energy density. The quantity  $\mathcal{V}(\psi)$  corresponds with the bulk free energy density of a spatially uniform system  $\psi = \text{const} \Rightarrow \nabla\psi = 0$ , since under these circumstances  $F/V = \mathcal{V}$ , where  $V$  is the total volume. In contrast, the *full* free energy density  $f$  also accounts for the free energy cost of spatial variations in the order parameter  $\psi$ . The quantity  $\psi$  is a suitable intensive variable of interest. The continuum integral in Eq. (1) can be thought of as a limit of a discrete sum over cells with fixed volumes, the cells tiling the space. Thus  $f$  must be regarded as a free energy computed at constant volume, insofar as the order parameter reflects density variations. Prominent examples of such types of free energy are given by the Helmholtz free energy  $A$ :

$$A = -k_B T \ln \sum_i e^{-E_i(V,N)/k_B T} \quad (2)$$

and the grand canonical free energy  $\Omega \equiv -pV$ :

$$\Omega \equiv -pV = -k_B T \ln \sum_i e^{-[E_i(V) - \mu N_i(V)]/k_B T}. \quad (3)$$

In the Helmholtz case, the summation is over all possible microstates  $i$  such that  $V_i = V$  and  $N_i = N$ , while in the grand-canonical case, the particle number  $N_i$  is unconstrained.<sup>1,21</sup> If, on the other hand, the degree of freedom of interest  $\psi$  is not strongly coupled to the density, as would be the case for the magnetization in a magnet, the volume integration in Eq. (1) largely amounts to a summation over sites hosting the degree of freedom and does not put limitation on the specific choice of free energy. An interesting example of the latter situation is represented by continuum mechanics<sup>22</sup>, even though the latter theory explicitly deals with deformations such as density changes. In continuum mechanics, the integration is over the volume of an *undeformed* sample and, thus, can be thought of as, essentially, a sum over lattice sites, not integration over actual space.

When the order parameter corresponds to a conserved quantity—such as the particle number—discontinuous phase transitions are signalled by the presence of a sign change in the second derivative  $\partial^2 \mathcal{V}/\partial \psi^2$ . Consider, for instance, the Helmholtz free energy of a spatially homogeneous van der Waals gas below the critical point, at fixed temperature and particle number. The free energy can be computed by formal integration  $A_2 = A_1 - \int_1^2 p dV$  of the van der Waals isotherm  $p = Nk_B T/(V - Nb) - a(N/V)^2$ , see sketch in Fig. 1(a). At any value of the volume  $V$  intermediate between the boundaries  $V_l$  and  $V_v$  of the non-concave region in the  $A(V)$  dependence, the system can lower its Helmholtz free energy by phase separating into vapor (mole fraction  $x_v = (V - V_l)/(V_v - V_l)$ ) and liquid (mole fraction  $x_l = (V_v - V)/(V_v - V_l) = 1 - x_v$ ). Upon phase separation, the dependence of the free energy on volume is given by the straight line  $A = x_v A_v + x_l A_l$ , which is the double tangent line that runs *under* the  $A(V)$  curve

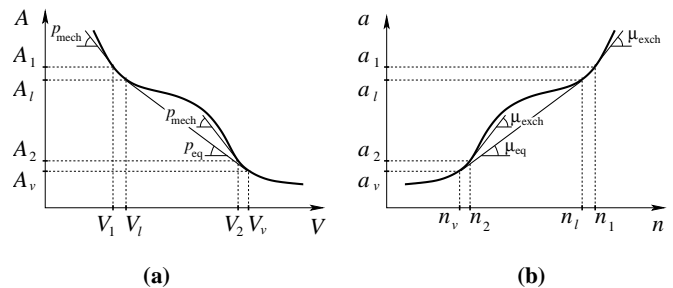


FIG. 1. **(a)** Sketch of the Helmholtz free energy  $A$  as a function of volume  $V$  of a liquid at constant temperature and particle number, below the critical point. The double tangent corresponds to the free energy of the phase separated system and is followed in equilibrium. While the two states 1 and 2 are in mechanical equilibrium, they are not in equilibrium with regard to particle exchange, unless  $p_{\text{mech}}$  is equal to the (negative) slope of the double tangent, whereby  $V_1 = V_l$  and  $V_2 = V_v$ . **(b)** Sketch of the Helmholtz free energy per unit volume,  $a \equiv A/V$ , as a function of particle concentration, at constant volume and temperature. States 1 and 2 are in equilibrium with respect to particle exchange, but not in mechanical equilibrium, unless  $\mu_{\text{exch}}$  is equal to the slope of the double tangent.

that was calculated under the assumption of complete spatial uniformity of the gas. We remind the reader that the Helmholtz free energy  $A = E - TS$  must be at its minimum at constant temperature and volume.<sup>1</sup> Viewed this way, the entropy  $S = -k_B \sum_i p_i \ln p_i$  ( $\sum_i p_i = 1$ ) is understood in its Gibbsian sense, where the probabilities  $p_i$  represent the statistical weights of microstates  $i$  and can be computed under a constraint of one's liking. The curved and flat  $A(V)$  segments at  $V_l < V < V_v$  in Fig. 1(a) are computed, respectively, with and without imposition of the constraint that the system be spatially homogeneous.

An infinite number of configurations 1 and 2 such that  $-\partial A/\partial V|_1 = -\partial A/\partial V|_2 \Rightarrow p_1 = p_2 \equiv p_{\text{mech}}$  correspond to a mechanical equilibrium, see the short, parallel tangents in Fig. 1(a). Yet only one of those configurations, viz.,  $(A_2 - A_1)/(V_2 - V_1) = \partial A/\partial V|_1 = \partial A/\partial V|_2$  also corresponds to *full* equilibrium, i.e., when the two parallel tangents strictly coincide thus implying  $V_1 = V_l$  and  $V_2 = V_v$ . Indeed, only at the corresponding pressure  $p_{\text{eq}} \equiv -(A_v - A_l)/(V_v - V_l)$  do the Gibbs free energies  $G = A + pV$  and, hence, the bulk chemical potentials of the two phases become equal:  $A_1 + p_1 V_1 = A_2 + p_2 V_2 \Rightarrow \mu_1 N = \mu_2 N$ , since  $G = \mu N$ .<sup>22</sup>

In the context of the density functional in Eq. (1), it is practical to vary the particle number at constant volume; density fluctuations are thus viewed as fluctuations of the particle number at fixed volume, not fluctuations of the local specific volume. The sketch in Fig. 1(b) of the Helmholtz free energy density  $a \equiv A/V$  as a function of concentration  $n = N/V$ , at constant volume, demonstrates that there are an infinite number of ways for two phases to co-exist in which there

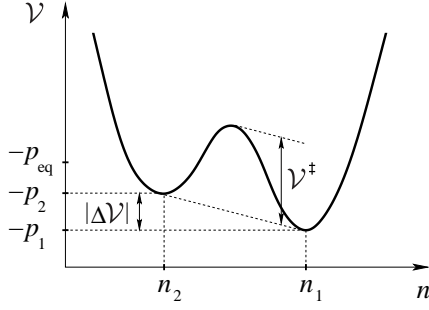


FIG. 2. Sketch of the bulk free energy density  $\mathcal{V}$  from Eq. (1), as could be obtained, for instance, from the Helmholtz free energy density by making the equilibrium state also the standard state. In the latter case, one sets  $\mathcal{V} = a - \mu_0 n$ , where  $a$  is the thick curve from Fig. 1(b), and  $\mu_0 = \mu_{\text{exch}}$ .

is no particle exchange between the phases:  $\partial a / \partial n|_1 = \partial a / \partial n|_2 \Rightarrow \mu_1 = \mu_2 \equiv \mu_{\text{exch}}$ . Yet only one of these configurations is also in *mechanical* equilibrium, so that  $(a_2 - a_1) / (n_2 - n_1) = \partial a / \partial n|_1 = \partial a / \partial n|_2$ . Hereby,  $A_1 - \mu_1 N_1 = A_2 - \mu_2 N_2 \Rightarrow -p_1 V = -p_2 V$ . At full equilibrium,  $\mu_1 = \mu_2 = (a_l - a_v) / (n_l - n_v) = \mu_{\text{eq}}$ .

The value of the chemical potentials  $\mu_1 = \mu_2$  in Fig. 1(b) has been chosen, for concreteness, so that the bulk vapor is oversaturated with respect to the liquid. The notion of the metastability of the vapor state becomes particularly vivid if one stipulates that either state 1 or 2 be the reference—or *standard*—state with regard to the chemical potential. (The choice of the standard state is, of course, arbitrary and is made according to one's convenience.) Formally, making state 1 the standard state is accomplished by using the free energy density  $\mathcal{V} \equiv a - \mu_0 n$  where the fixed quantity  $\mu_0$  is numerically equal to the chemical potential at concentration  $n_1$  (or  $n_2$ ) according to the original Helmholtz free energy  $\mu_0 = \partial a / \partial n|_{n_1} = \partial a / \partial n|_{n_2}$ . The equilibrium values of the concentration—stable or metastable—thus correspond to the minima of the function  $\mathcal{V}$  by construction:  $\partial \mathcal{V} / \partial n|_1 = \partial \mathcal{V} / \partial n|_2 = 0$ . The free energy density  $\mathcal{V}$  corresponding to Fig. 1(b) is sketched in Fig. 2. One can alternatively think of  $\mu_0$  as an externally imposed chemical potential. Hereby, the actual (bulk) chemical potential  $\mu$  is equal to  $\mu_0$  only in equilibrium, i.e., at the minima of  $\mathcal{V}$ . Because at the minima,  $\mathcal{V}(n) = (A - \mu_0 N) / V = (A - \mu N) / V = -p$ , the depths of the minima of  $\mathcal{V}$  are numerically equal to the negative pressure. Note that when the vapor and liquid are in equilibrium with respect to particle exchange but not in mechanical equilibrium, as in Fig. 2, the pressure is always greater in the undersaturated phase, as expected, while the magnitude of the deviation  $|p - p_{\text{eq}}|$  from the equilibrium value  $p_{\text{eq}}$  is always greater in the denser phase.

The free energy density in Fig. 2 is a typical example of the free energy density  $\mathcal{V}$  from Eq. (1) in the context of a *discontinuous* phase transition. Hereby, the order parameter has distinct values in the distinct phases of

interest; the two phases correspond to the two minima of the function  $\mathcal{V}$ , which are separated by a barrier. Another common example of a conserved order parameter is magnetization, call it  $\mathcal{M}$ . In this case, the role of the chemical potential  $\mu$  is played by the externally imposed magnetic field  $h$ , since  $dA = -SdT + h d\mathcal{M}$ . The transition itself amounts to a reversal of the magnetization of a magnet cooled below its Curie point. In the rest of the paper, we largely limit ourselves to fluid mixtures made of  $M$  components whose concentrations we denote with  $n_i$ ,  $i = 1 \dots M$ .

We specifically allow the coefficient  $\kappa$  at the square gradient term in Eq. (1) to explicitly depend on the order parameters. (The dependence of  $\kappa$  on the coordinate is thus exclusively through the coordinate dependence of the order parameter, if any.) This coefficient directly reflects particle-particle interactions and thus generally differs between distinct phases of matter. Specifically, the coefficient  $\kappa$  (for a pure substance) scales linearly with the direct correlation function  $c(\mathbf{r}_1, \mathbf{r}_2) \equiv -\beta \delta^2 F_{\text{ex}}[n(\mathbf{r})] / \delta n(\mathbf{r}_1) \delta n(\mathbf{r}_2)$ , where the derivative is evaluated at equilibrium density and  $F_{\text{ex}}$  is the non-ideal portion of the free energy. The direct correlation function in a fluid generally scales with the bulk modulus and thus sensitively depends on the density and temperature. Explicit calculations for the coefficient  $\kappa$  can be found in Refs.<sup>23,24</sup>

We thus adopt the following Landau-Ginzburg functional:

$$F(\{n_i(\mathbf{r})\}) = \int d^3 \mathbf{r} \left[ \sum_{ij}^M \frac{\kappa_{ij}}{2} (\nabla n_i \nabla n_j) + \mathcal{V}(\{n_i\}) \right] \quad (4)$$

where the summation is over distinct chemical species. The matrix  $\kappa_{ij}$  is automatically symmetric,  $\kappa_{ij} = \kappa_{ji}$ , and, also, positive-definite by construction.

The free energy of the configuration  $n_i(\mathbf{r}) + \delta n_i(\mathbf{r})$  within a connected region, relative to that of configuration  $n_i(\mathbf{r})$ , is given to the first order in a (small) quantity  $\delta n_i$  by the expression:

$$\begin{aligned} \delta F &\equiv F(\{n_i + \delta n_i\}) - F(\{n_i\}) \\ &= \sum_{ij} \int_S (d\mathbf{S} \nabla n_j) \kappa_{ij} \delta n_i + \sum_i \int_V dV \mu_i \delta n_i, \end{aligned} \quad (5)$$

where the first and second integrals are over the boundary and the bulk of the region, respectively, and

$$\mu_i(\mathbf{r}) = \frac{\partial \mathcal{V}}{\partial n_i} - \sum_j \nabla (\kappa_{ij} \nabla n_j) + \frac{1}{2} \sum_{lm} \frac{\partial \kappa_{lm}}{\partial n_i} (\nabla n_l \nabla n_m). \quad (6)$$

By Eq. (5), the quantity

$$\mu_i(\mathbf{r}) = \frac{\delta F}{\delta n_i(\mathbf{r})}. \quad (7)$$

It thus equals the free energy cost of adding a particle to the system at point  $\mathbf{r}$ , i.e., the local chemical potential. We see from Eq. (6) that in addition to the obvious



contribution  $\partial\mathcal{V}/\partial n_i$ , the local chemical potential also exhibits contributions due to the free energy cost of density variations.

If the local cost of adding a particle is not spatially homogeneous, particle fluxes will emerge spontaneously. In spatial dimensions three and higher, phenomenological Fick's law can be used to connect the particle fluxes  $\mathbf{j}_i$  and the gradients of the chemical potentials of the species present:

$$\mathbf{j}_i = - \sum_j \tilde{D}_{ij} \nabla \mu_j, \quad (8)$$

where the symmetric<sup>25–27</sup> matrix  $\tilde{D}_{ij}$  represents a set of self-diffusion coefficients. These quantities are generally concentration-dependent and can be related to the regular diffusivities through compressibilities. For instance, Eq. (8) yields for a pure substance near equilibrium:  $\mathbf{j} = -\tilde{D}(\partial\mu/\partial n)\nabla n$ , while  $(\partial\mu/\partial n) = v^2/\kappa_T$ , where  $\kappa_T$  and  $v$  are the compressibility and specific volume respectively. Consequently, the ordinary diffusivity  $D_{\text{diff}} = \tilde{D}v^2/\kappa_T$ .

Eq. (8), together with particle conservation  $\dot{n}_i = -\nabla \cdot \mathbf{j}_i$ , allows one to write down a system of equations governing relaxation of the system toward equilibrium<sup>12</sup>:

$$\dot{n}_i = \sum_j \nabla \cdot (\tilde{D}_{ij} \nabla \mu_j), \quad (9)$$

with  $\mu_i$  from Eq. (6).

By Eq. (8), the chemical potential must be spatially uniform in full equilibrium:

$$\mu_i = \text{const} = 0, \text{ in equilibrium}, \quad (10)$$

where we have used that steady state is also the standard state, by construction. However, the condition for *local* steady state is much less restrictive. According to Eq. (9), one must only require that  $\sum_j \nabla \cdot (\tilde{D}_{ij} \nabla \mu_j) = 0$ , which allows for spatially varying chemical potentials.

To avoid confusion, we note that Eq. (9) is incomplete in two ways, in addition to being phenomenological. For one thing, it does not account for advection, which is generally present in mixtures.<sup>12</sup> Indeed, an individual component can flow also with the mixture as a whole, not only by itself. Still, this complication does not arise in steady state, when there is no net flow. Also, Eqs. (9) should properly contain terms accounting for thermal noise<sup>28</sup> to describe processes other than relaxation toward equilibrium.

Although less common, non-conserved order parameters are encountered in applications too. In the absence of a conservation law for the order parameter, one often uses the empirical Landau-Onsager ansatz<sup>1,12,25,26,29</sup> for the time evolution of the system:<sup>30</sup>

$$\dot{\psi} = -\mathcal{K} \frac{\delta F}{\delta \psi}. \quad (11)$$

Eq. (11) is the simplest empirical law one can write down that relates the rate of relaxation toward or away from steady state to the deviation  $\delta\psi(\mathbf{r}) \equiv \psi(\mathbf{r}) - \psi_0(\mathbf{r})$  of the order parameter  $\psi(\mathbf{r})$  from its steady-state value  $\psi_0(\mathbf{r})$  that optimizes the functional:  $\delta F/\delta\psi|_{\psi_0} = 0$ . Finally note that Eqs. (7) and (10) on the one hand and Eq. (11) on the other hand imply the equations determining the steady state themselves are identical for conserved and non-conserved order parameters, even though relaxation toward or away from steady state is governed by distinct laws in the two cases.

### III. PRESSURE IN THE LANDAU-GINZBURG FUNCTIONAL

Stationary points of the functional that are also *minima* correspond to a spatially uniform system residing wholly in a specific phase. Such a free energy minimum will be either stable or metastable according to whether the corresponding minimum in the bulk free energy density  $\mathcal{V}(\psi)$  is stable or metastable. In the following, we will be discussing additional stationary points of the functional that correspond not to minima but to *saddle points*. Such saddle points, if any, are transition-state configurations that could arise during a phase transition between two phases. Specifically, we consider *droplet* configurations such that the order parameters achieve their bulk values  $n_i^{(\text{out},b)}$  in the majority phase, at infinity. We demand that near the origin, the mixture is on the other side of the transition state of the bulk free energy density  $\mathcal{V}$ , i.e., in the minority phase.

In the limit of thin interface, the transition-state droplet configuration is obviously spherically symmetric, since this configuration minimizes the surface area for a given volume of the droplet. Alternatively said, such spherically-symmetric configuration satisfies Pascal's law within individual phases because it insures uniformity of pressure (separately) on the inside and outside. Below we assume that the bulk free energy density does not explicitly depend on the coordinate,  $\partial\mathcal{V}/\partial\mathbf{r} = 0$ , unless explicitly stated otherwise. Now, when the interface is not thin, it appears difficult to make general statements about the symmetry of the droplet solution because Eqs. (10) are non-linear. Still, inasmuch as we expect the lowest free energy saddle point to be unique we can also expect the corresponding solution to be spherically symmetric. Indeed, suppose on the contrary that the solution is only of *discrete* symmetry with respect to rotations. Further, suppose for the sake of argument that this solution transforms under the corresponding symmetry operations in the same way as the coordinate  $x$ . For each such solution, there will be also two other solutions, transforming as the coordinates  $y$  and  $z$  respectively, which contradicts the original assumption that the solution is unique. Cylindrically—but not spherically—symmetric solutions can be dismissed by the same token. The following boundary conditions thus apply to spheri-

cally symmetric droplets:

$$\begin{aligned} n_i(\mathbf{r} = \infty) &= n_i^{(\text{out},b)} \\ \nabla n_i(\mathbf{r} = 0) &= 0. \end{aligned} \quad (12)$$

The actual values of the order parameters may not reach their bulk values  $n_i^{(\text{in},b)}$  in the minority phase. However in view of the reflection symmetry of the problem, their spatial derivatives must vanish at the origin to avoid a discontinuity.

In the presence of spherical symmetry, Eq. (6) yields in  $D$  spatial dimensions:

$$\begin{aligned} \sum_j \kappa_{ij} \left( \frac{d^2 n_j}{dr^2} + \frac{D-1}{r} \frac{dn_j}{dr} \right) \\ = \frac{\partial \mathcal{V}}{\partial n_i} - \sum_j \frac{d\kappa_{ij}}{dr} \frac{dn_j}{dr} + \frac{1}{2} \sum_{lm} \frac{\partial \kappa_{lm}}{\partial n_i} \frac{dn_l}{dr} \frac{dn_m}{dr} - \mu_i. \end{aligned} \quad (13)$$

Note the dependence of  $\kappa_{ij}$  on the coordinate is exclusively through the coordinate dependences of the concentrations.

Multiplying Eq. (13) by  $dn_i$ , summing over  $i$ , and integrating from some point 1 to point 2 yields:

$$\begin{aligned} \sum_{ij} \left. \frac{\kappa_{ij}}{2} \frac{dn_i}{dr} \frac{dn_j}{dr} \right|_1^2 - \mathcal{V}|_1^2 \\ = -(D-1) \int_1^2 \frac{dr}{r} \sum_{ij} \kappa_{ij} \frac{dn_i}{dr} \frac{dn_j}{dr} - \sum_i \int_1^2 \mu_i dn_i. \end{aligned} \quad (14)$$

In deriving the above equation, we have taken advantage of the symmetry of the  $\kappa_{ij}$  matrix. One immediately observes that when  $D = 1$ , i.e., for a flat interface, and in complete equilibrium,  $\mu_i = 0$ , the following quantity is conserved:

$$\sum_{ij} \frac{\kappa_{ij}}{2} \frac{dn_i}{dr} \frac{dn_j}{dr} - \mathcal{V} = \text{const}, \quad D = 1, \mu_i = 0. \quad (15)$$

This is expected based on the formal correspondence between the free energy function (4) in the  $D = 1$ ,  $\mu_i = 0$  case and the action in classical mechanics,<sup>31</sup> i.e.  $\int dt [\sum_{ij} M_{ij} \dot{x}_i \dot{x}_j / 2 - U(x_i)]$ . Hereby, the concentrations  $n_i$  are the analogs of the mechanical coordinates  $x_i$ , the coordinate  $x$  of time  $t$ , and the bulk free energy density  $\mathcal{V}$  of the negative potential energy  $-U$ . The conserved quantity (15) is thus formally analogous to energy in mechanics.

Taking the above, formal correspondence with mechanics a step further, we note that the mechanical energy is the partial (not full!) derivative of the mechanical action with respect to time, with the minus sign.<sup>31</sup> We can use this notion to establish that the analog of the mechanical energy in the present context is actually the *mechanical pressure*. The latter statement turns out to be correct not only in 1D, but, more generally, in any number of dimensions so long as the steady state solution is spherically

symmetric. Indeed, consider first an arbitrary droplet geometry. It will be convenient to switch to a modified free energy function  $\tilde{F}$ :

$$\tilde{F}(\{n_i\}) \equiv F - \sum_i \int \mu_i n_i dV = \int (f - \sum_i \mu_i n_i) dV, \quad (16)$$

where  $\mu_i$ 's are now regarded as some preset functions of the coordinate  $\mathbf{r}$ . The quantity  $f$  is the Helmholtz free energy density corresponding to the functional in Eq. (4). The free energy of the configuration  $n_i(\mathbf{r}) + \delta n_i(\mathbf{r})$  within a connected region, relative to that of configuration  $n_i(\mathbf{r})$ , is given to the first order in a (small) quantity  $\delta n_i$  by the expression:

$$\begin{aligned} \delta \tilde{F} &\equiv \tilde{F}(\{n_i + \delta n_i\}) - \tilde{F}(\{n_i\}) \\ &= \sum_{ij} \int_S (d\mathbf{S} \cdot \nabla n_j) \kappa_{ij} \delta n_i + \sum_i \int_V dV \left( \frac{\delta F}{\delta n_i} - \mu_i \right) \delta n_i. \end{aligned} \quad (17)$$

We now limit our attention to those specific concentration profiles that satisfy Eq. (7). For those specific profiles, the function  $\tilde{F}$  is actually a Legendre transform of the functional  $F$ , namely, the grand-canonical free energy as defined for a coordinate-dependent chemical potential:

$$\Omega(\{\mu_i\}) \equiv F - \sum_i \int \mu_i n_i dV \quad (18)$$

Under these circumstances, the volume integral vanishes in Eq. (17); one may present the free energy variation as an integral over the sample's boundary.

Let us now choose as our boundary an *isobaric* surface, or surface of constant pressure. This way, the hydrostatic forces near the boundary are exactly normal to the latter. Varying the free energy with respect to the displacement  $l$  along the normal to the surface at a specific location thus simply yields the negative pressure at that location times the area  $S$  of the (small) patch over which the variation is performed:

$$\frac{1}{S} \left( \frac{\partial \Omega}{\partial l} \right)_{T, \mu_i} = \left( \frac{\partial \Omega}{\partial V} \right)_{T, \mu_i} = -p. \quad (19)$$

On the other hand, by the chain rule of differentiation:

$$\frac{d\tilde{F}}{dl} = \frac{\partial \tilde{F}}{\partial l} + \sum_i \int_S dS(\mathbf{r}) \frac{\delta \tilde{F}}{\delta n_i(\mathbf{r})} \frac{dn_i(\mathbf{r})}{dl}, \quad (20)$$

where  $\delta \tilde{F} / \delta n_i(\mathbf{r})$  is the functional derivative of the free energy with respect to the concentration  $n_i(\mathbf{r})$  at point  $\mathbf{r}$  belonging to the boundary. According to Eqs. (17) and (7), this derivative is given by the expression  $\sum_j \kappa_{ij} (\mathbf{e}(\mathbf{r}) \cdot \nabla n_j)$ , where  $\mathbf{e}(\mathbf{r}) \equiv d\mathbf{S}(\mathbf{r}) / dS(\mathbf{r})$  is the external normal to the boundary at the point  $\mathbf{r}$ ,  $e^2 = 1$ . Note that  $dn_i / dl = (\mathbf{e}(\mathbf{r}) \cdot \nabla n_i)$ . Finally, the full derivative  $d\tilde{F} / dl$  is simply given by the integrand in Eq. (16) integrated over the patch, according to the Newton-Leibniz

formula. Putting these notions together, while taking the limit  $S \rightarrow 0$ , yields the following formula for the pressure in the Landau-Ginzburg functional:

$$p = -\mathcal{V} + \sum_i \mu_i n_i + \sum_{ij}^M \kappa_{ij} \left[ (\mathbf{e} \nabla n_i)(\mathbf{e} \nabla n_j) - \frac{1}{2} (\nabla n_i \nabla n_j) \right], \quad (21)$$

where  $\mathbf{e} \equiv d\mathbf{S}/dS$ , as before. Note the above equation is invariant with respect to the choice of the standard state for the chemical potential, as it should be.

Eq. (21), by itself, cannot be used to determine the pressure in arbitrary geometries, unless the orientation of the isobaric surface happens to be known. Some insight may be already gleaned, however, when the  $\kappa_{ij}$  matrix is diagonal, in which case it is easy to write an upper bound for the pressure that does not depend on that orientation:

$$p \leq -\mathcal{V} + \sum_i \mu_i n_i + \sum_{ij}^M \frac{\kappa_{ij}}{2} (\nabla n_i \nabla n_j), \text{ if } \kappa_{ij} = \kappa_i \delta_{ij}. \quad (22)$$

Note that Eqs. (17)-(22) also apply when the bulk free energy density  $\mathcal{V}$  explicitly depends on the coordinate.

Fortunately, an explicit expression for pressure can be obtained in the presence of spherical symmetry, whereby the isobaric surfaces also coincide with the surfaces of constant concentrations and chemical potentials. Consequently, the gradients  $\nabla n_i$  are strictly parallel to the external normal  $\mathbf{e}$  and so Eq. (21) yields:

$$p(r) = -\mathcal{V} + \sum_i \mu_i n_i + \sum_{ij} \frac{\kappa_{ij}}{2} \frac{dn_i}{dr} \frac{dn_j}{dr}, \quad (23)$$

c.f. Eq. (22). We thus observe that the quantity (15), which is conserved for flat interfaces (when  $\mu_i = 0$ ), corresponds with the mechanical pressure. The spatial homogeneity of pressure for a flat interface—and, hence, during *macroscopic* phase coexistence—is, of course, the familiar Pascal's law.

Thus, Eqs. (14) and (23) yield for an equilibrium flat interface perpendicular to the  $x$  axis:

$$p = -\mathcal{V} + \sum_{ij} \frac{\kappa_{ij}}{2} \frac{dn_i}{dx} \frac{dn_j}{dx} = \text{const}, \quad D = 1, \mu_i = 0. \quad (24)$$

One may think of this equation as saying that the variation in the order parameter exactly compensates for the decrease in pressure, due to the bulk free energy term  $\mathcal{V}$ , that arises in the transition state. This is not unlike how the variation in the chemical potential, due to the bulk free energy term, is exactly compensated by the spatial variation in the order parameter in Eqs. (6) and (10). No such pressure compensation takes place in spatial dimensions greater than one, however, for which Eqs. (14) and (23) yield:

$$p_2 - p_1 = -(D-1) \int_1^2 \frac{dr}{r} \sum_{ij} \kappa_{ij} \frac{dn_i}{dr} \frac{dn_j}{dr} + \sum_i \int_1^2 n_i d\mu_i. \quad (25)$$

This is a generalization of a result first obtained by van der Waals<sup>4</sup> for a single-component substance and a constant  $\kappa$  to mixtures, concentration-dependent coefficients  $\kappa_{ij}$ , and off-equilibrium situations in the sense that  $\mu_i \neq 0$ . Another way to look at formula (25) is to recall that in an equilibrated, uniform sample,  $G = \sum_i \mu_i N_i$  while  $dG = -SdT + Vdp + \sum_i \mu_i dN_i$ . At constant temperature and volume, this yields  $p_2 - p_1 = \sum_i \int_1^2 n_i d\mu_i$  for any pair of equilibrium states 1 and 2. According to Eq. (25), such two states can be representative of the very same sample, however the expression for the pressure difference must be corrected for a finite curvature of density variation patterns, if any.

Now choose points 1 and 2 at the center of the droplet and infinity, respectively. In view of positive-definiteness of the matrix  $\kappa_{ij}$ , Eq. (25) shows that pressure always increases monotonically toward the center of a spherical droplet in full equilibrium. (We remind the reader that the equilibrium may be unstable, as is the case with critical nuclei.) Furthermore, in the limit of infinitely weak undersaturation of the minority phase,  $\Delta\mathcal{V} \rightarrow 0$ , the expression for the excess pressure inside the droplet, relative to the bulk, reduces to the venerable Laplace form. Indeed, sufficiently close to macroscopic coexistence of the two phases, the droplet size can be made arbitrarily larger than the interface width. The latter width must be finite and, in fact, is limited by its value during macroscopic co-existence: According to Eq. (14), the derivatives  $dn_i/dr$  become only larger when  $D > 1$ . On the other hand, the interface width during macroscopic coexistence is finite because otherwise, the system could always lower its free energy by an infinite amount, by locally “falling” into one of the two minima in Fig. 2. Under these circumstances, the order parameters differ from their (spatially-uniform) values in the bulk phases in a spatial interval that can be made arbitrarily narrower than the droplet size. Consequently one can unambiguously define a droplet radius  $R$ . Because the derivatives  $dn_i/dr$  have appreciable magnitudes only within a finite interval, the  $1/r$  factor in the integrand of Eq. (14) can be taken outside the integral, while the integral itself can be replaced by the value it achieves in macroscopic equilibrium,  $\Delta\mathcal{V} = 0$ , i.e., for a flat interface. Further, Eq. (15) implies that the integral is in fact equal to the excess free energy of the flat interface, relative to the spatially uniform state, per unit area. This integral is thus equal to the surface tension coefficient  $\sigma$ :

$$\sigma = \int_{-\infty}^{\infty} dx \sum_{ij} \kappa_{ij} \frac{dn_i}{dx} \frac{dn_j}{dx} = \int_{-\infty}^{\infty} dx (\mathcal{V} - \mathcal{V}_{\infty}), \quad (26)$$

where, we remind,  $\Delta\mathcal{V} = 0$ . Thus according to this argument and Eq. (25), for any two points 1 and 2 inside and outside the droplet respectively, we obtain the venerable Laplace's formula  $p_1 = p_2 + (D-1)\sigma/R$ . This result, combined with Fig. 1(b) yields two classic notions: On the one hand, the minority phase must be undersaturated relative to the majority phase. On the other hand, the result allows one to estimate the deviation of

pressure in either phase compared to its value during macroscopic coexistence, which then yields the venerable Gibbs-Thompson formula.<sup>1</sup>

For a single-component fluid, Eq. (26) can be significantly simplified:<sup>6</sup>

$$\sigma = \int_{n_{\min,1}}^{n_{\min,2}} dn \sqrt{2\kappa(\mathcal{V} - \mathcal{V}_\infty)}, \quad (27)$$

where  $n_{\min,1}$  and  $n_{\min,2}$  correspond to the two minima of the bulk free energy  $\mathcal{V}(n)$ ;  $n_{\min,1} < n_{\min,2}$  by construction. The above expression is remarkable in that it allows one to compute the surface tension coefficient (for a flat interface) without the need to solve Eq. (10). By Eq. (27), the surface tension coefficient is determined, generically, by the height  $\mathcal{V}^\ddagger$  of the barrier in the bulk free energy term, see Fig. 2, and the value of the coefficient  $\kappa$  around the transition state:  $\sigma \simeq \sqrt{\kappa^\ddagger \mathcal{V}^\ddagger}$ . The corresponding length scale, which reflects the interface width, is  $l \simeq \sqrt{\kappa^\ddagger / \mathcal{V}^\ddagger}$ , and the surface tension coefficient is simply  $\sigma \simeq \mathcal{V}^\ddagger l$ . Some contributions to both the interface width and the surface tension coefficient are expected from the order parameter fluctuations near the minima. The corresponding lengthscale is proportional to  $[\kappa / (\partial^2 \mathcal{V} / \partial n^2)]^{1/2}$ . These contributions, however, must not be very significant, otherwise the system must be regarded as being close to criticality, in which case the mean-field Landau-Ginzburg functional becomes inadequate either quantitatively or, sometimes, even qualitatively.

In a mixture, the surface tension coefficient can still be presented as a line integral connecting the free energy minima that correspond with the phases in question, in the  $\{n_i\}$  space. This is obvious from the l.h.s. equation of Eq. (26). While the resulting expression allows one to decompose the overall mismatch free energy into contributions from individual components, it requires one to first solve Eq. (10), which is generally not a simple task.

#### IV. SINGULAR BULK FREE ENERGY DENSITY. STEADY STATE SOLUTION.

Equations (10) are non-linear because generally, the bulk free energy  $\mathcal{V}$  is not a quadratic or linear function of the concentrations while the coefficients  $\kappa_{ij}$  may have distinct values between the phases and interfacial regions. Although the equations can be solved numerically, avoiding numerical instabilities requires extra effort. Since the actual functional form of  $\mathcal{V}$  and  $\kappa_{ij}$ 's are usually not known in the first place, a practical strategy is to make  $\mathcal{V}$  a quadratic function of the concentrations  $n_i$  everywhere in the  $\{n_i\}$  space except in a subspace of lower dimensions. And so for each phase  $\alpha$ :

$$\mathcal{V}^{(\alpha)} = \sum_{ij} \frac{m_{ij}^\alpha}{2} (n_i - n_i^{(\alpha,b)})(n_j - n_j^{(\alpha,b)}) + \mathcal{V}^{(\alpha,b)}, \quad (28)$$

where  $n_i^{(\alpha,b)}$  denotes the bulk value of the concentration of component  $i$  in phase  $\alpha$  and the symmetric matrix  $m_{ij}$  is positive definite. The quantity  $\Delta\mathcal{V} \equiv \mathcal{V}^{(\text{in},b)} - \mathcal{V}^{(\text{out},b)}$  thus gives the bulk free energy difference, per unit volume, between the two phases, see Fig. 2. For two co-existing phases, the bulk free energy  $\mathcal{V}$  consists of two paraboids. If one chooses the phase boundary (in the  $\{n_i\}$  space) as the intersection of the paraboids, see illustration in Fig. 3, the resulting bulk free energy experiences a discontinuity in the gradient. Otherwise, the discontinuity is in the function itself. The functional form (28) presents some limitations in terms of modelling because it does not allow one to vary the curvatures of the bulk free energy surface in pure phases independently from the height of the barrier separating the minima corresponding to the pure phases. This effectively implies that the lengthscales  $\sqrt{\kappa/m}$  and  $\sqrt{\kappa^\ddagger/\mathcal{V}^\ddagger}$ , discussed above, are not independent. Yet we shall see that even this simplified form of  $\mathcal{V}$  captures the essential features of thick interfaces that are not accessible to the thin-wall approximation of the classical nucleation theory.

A trajectory in the  $\{n_i\}$  space corresponding to droplet configurations crosses the phase boundary in that space exactly once; trajectories with more crossings automatically correspond to higher free energies. As a result, the *physical* space is divided into two parts separated by a sharp spherical boundary at some radius  $r = R$ , the inside and outside parts corresponding to the minority and majority phase respectively. Likewise, one may regard  $\kappa_{ij}$ 's as constant in each phase but assume they may experience a discontinuous jump at the phase boundary. Under these circumstances, Eqs. (10) become linear within individual phases:

$$\sum_j \kappa_{ij} \nabla^2 n_j = \sum_j m_{ij} (n_j - n_j^{(b)}) \quad (29)$$

while the following boundary conditions must be specified at the dividing surface:

$$n_i(R^+) = n_i(R^-) \equiv n_i^\ddagger \quad (30)$$

$$\left( \sum_{ij} \frac{\kappa_{ij}}{2} \frac{dn_i}{dr} \frac{dn_j}{dr} - \mathcal{V} \right) \bigg|_{R^-}^{R^+} = 0 \quad (31)$$

The first set of conditions, Eq. (30), ensures continuity of the concentrations at the dividing surface. These conditions are chosen based on the physical consideration that in a fluid, molecules must be able to exchange positions and so a fluid can be only defined within a finite region, even if very small. Consequently, the concentration must change *continuously* in space. To give a counterexample, the effective interface between a *solid* and the corresponding vapor can be made arbitrarily narrow sufficiently below the triple point.

The second condition, Eq. (31), which places a constraint on the concentration gradients at the dividing surface, stems from Eq. (14). According to Eq. (23), the



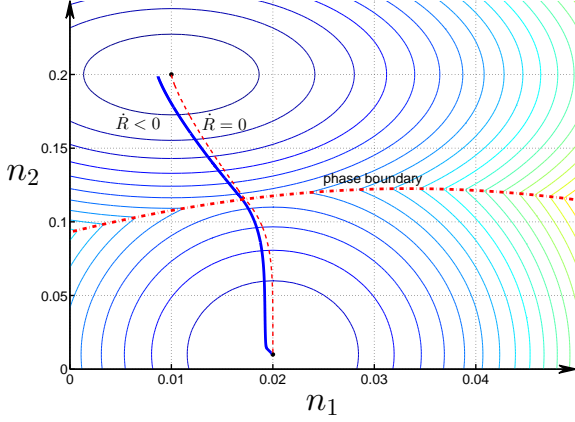


FIG. 3. Contour plot of the bulk free energy density  $\mathcal{V}(n_1, n_2)$  as a function of the concentrations  $n_1$  and  $n_2$  of the components of a binary mixture. The upper-left minimum corresponds with the undersaturated, minority phase. The two “trajectories” correspond to the density profiles of the two droplet solutions that are illustrated in detail in Fig. 4. The parameters employed in this Section are as follows:  $\kappa_{11}^{\text{in}} = 2000$ ,  $\kappa_{22}^{\text{in}} = 300$ ,  $\kappa_{11}^{\text{out}} = 20$ ,  $\kappa_{22}^{\text{out}} = 15$ ,  $\kappa_{12} = 0$ ,  $m_{11}^{\text{in}} = 400$ ,  $m_{11}^{\text{out}} = 700$ ,  $m_{22}^{\text{in}} = 40$ ,  $m_{22}^{\text{out}} = 20$ ,  $m_{12} = 0$ ,  $n_1^{(\text{in},b)} = 0.01$ ,  $n_2^{(\text{in},b)} = 0.2$ ,  $n_1^{(\text{out},b)} = 0.02$ ,  $n_2^{(\text{out},b)} = 0.01$ ,  $\tilde{D}_{12} = 0$ ,  $\tilde{D}_{ii}m_{ii} = 1$  for  $i = 1, 2$  in both phases,  $\Delta\mathcal{V} = -0.04$ . The units are arbitrary; as a rough guide, the unit of length is set at molecular dimensions and the unit of energy at a small fraction of  $k_B T$ .

condition in Eq. (31) corresponds with the continuity of pressure. This is required so that there is a balance of microscopic forces at each point in space, as mentioned in the Motivation. Conversely, if the boundary condition (31) is not obeyed, the solution of Eq. (10) yields  $\mathcal{V}[n_i(-\infty)] \neq \mathcal{V}[n_i(+\infty)]$  for a flat interface, that is, two macroscopic phases in thermodynamic equilibrium are not in mechanical equilibrium, thus leading to a contradiction.

Note that there are no separate constraints on individual concentration gradients; such constraints could be thought of as some matching conditions with regard to *partial* pressures of the components, between the two phases. Only in a pure substance, does Eq. (31) place a hard constraint on the concentration gradient. In any event, we observe that when the coefficients  $\kappa_{ij}$  experience a jump across the inter-phase boundary, so do generally the concentration gradients and hence the quantities  $\sum_j \kappa_{ij} (dn_j/dr)$ . In the aforementioned mechanics analogy, each quantity  $\sum_j \kappa_{ij} (dn_j/dr)$  corresponds with a momentum:  $\partial f / \partial (dn_i/dr) = \sum_j \kappa_{ij} (dn_j/dr)$ . The present results are a consequence of the Nöther theorem: In the mechanics analogy, the concentration-dependent  $\kappa_{ij}$ ’s correspond to coordinate-dependent masses. For a Lagrangian that depends explicitly on the coordinate but not on time, the energy is still conserved, but not the momentum. We reiterate that within the formal analogy

between the Landau-Ginzburg density functional theory and the Lagrange formulation of mechanics, Pascal’s law corresponds to energy conservation.

For concreteness, choose the dividing surface at the intersection of the two paraboloids  $\mathcal{V}^{(\text{in})}$  and  $\mathcal{V}^{(\text{out})}$ , see Eq. (28), corresponding to the phases inside and outside the droplet respectively:

$$\mathcal{V}^{(\text{in})}(\{n_i^\dagger\}) = \mathcal{V}^{(\text{out})}(\{n_i^\dagger\}), \quad (32)$$

while assuming that the coefficients  $\kappa_{ij}$  may experience a discontinuity also at the very same surface. Under these circumstances, the boundary condition (31) simply states that the dynamic term of the free energy functional (4) must be continuous across the dividing surface:

$$\sum_{ij} \frac{\kappa_{ij}}{2} \frac{dn_i}{dr} \frac{dn_j}{dr} \Big|_{R^-}^{R^+} = 0. \quad (33)$$

Eqs. (30), (31), and (32) together represent  $M + 2$  constraints.

While natural, the choice of boundary in Eq. (32) is not obligatory. If the boundary is chosen so that the bulk free energy density is *discontinuous*, then the most general boundary condition from Eq. (31) must be used. If the discontinuity in the coefficients  $\kappa_{ij}$  takes place at concentration values other than the dividing surface for the bulk free energy density, there will be another dividing surface in real space. The present methodology can be straightforwardly extended to such situations.

Now, the linear equations (29), subject to the boundary conditions (12) are solved by the following functions, except in certain degenerate cases that can be handled straightforwardly:

$$n_i = \begin{cases} n_i^{(\text{out},b)} + \sum_{jl} C_l^{(j)} e^{-k_l r} / r, & r \geq R \\ n_i^{(\text{in},b)} + \sum_{jl} C_l^{(j)} \sinh(k_l r) / r, & r < R, \end{cases} \quad (34)$$

where the coefficients  $C_l^{(j)}$  and parameters  $k_l$  satisfy the following equations (for each  $i$  and phase):

$$\sum_j^M C_l^{(j)} (\kappa_{ij} k^2 - m_{ij}) = 0. \quad (35)$$

Since the characteristic equation  $\text{Det}(\kappa_{ij} k^2 - m_{ij}) = 0$  has  $M$  roots, one can pick at most  $M$  linearly independent vectors  $C^{(j)}$  (each of which has  $M$  components). Consequently, the values of the coefficients at one harmonic determines the coefficients for the rest of the harmonics. Thus there are only  $M$  independent coefficients  $C_l^{(j)}$  in each phase. Together with the radius  $R$ , which must be determined self-consistently, there are  $2M + 1$  unknowns.

We thus have  $(2M + 1) - (M + 2) = M - 1$  unknowns to be determined, which is exactly the dimensionality of

the dividing surface in the  $\{n_i\}$  space. It is convenient to take the values of the transition state concentrations  $n_i^\ddagger$ ,  $i = 1, \dots, (M-1)$ , as the unknowns. The reason why the problem is so far underdetermined is that we have solved for stationary-state configurations within individual phases but not *at* the interface. Writing down equations at the phase boundary would require one to separately specify the behavior of the coefficients  $\kappa_{ij}$  and the bulk free energy  $\mathcal{V}$  in that region. A quick way to see that the number  $(M-1)$  of undetermined variables actually makes sense is to pretend that the components could chemically interconvert at the interface. In the presence of such interconversion, there would be imposed exactly  $(M-1)$  constraints on the concentrations  $n_i^\ddagger$ . (There are  $M$  equations,  $\dot{n}_i^\ddagger = 0$ , of which one is automatically satisfied because of particle conservation.) Instead of explicitly treating dynamics at the interface, we note that since equations (10) constitute a free energy optimization problem, the steady state configuration can be determined by minimizing the free energy function (4)—as computed using the concentration profiles (34)—with respect to the undetermined quantities, i.e., the concentrations  $n_i^\ddagger$ ,  $i = 1, \dots, (M-1)$  at the phase boundary. Simply stated, these  $(M-1)$  variables fully specify the chemical composition at the interface.

The above methodology can be straightforwardly extended to a non-stationary case, namely, a spherically symmetric droplet that is evaporating or growing; some caveats will apply. According to the above discussion, a droplet whose radius  $R$  is greater or less than its stationary, critical value will grow indefinitely and evaporate, respectively. One may make a steady-state approximation, by which the concentrations within the phases are assumed to equilibrate much faster than the droplet growth/decay. Generically, such an approximation is adequate when  $\dot{R}/R \ll D_{\text{diff}}/R^2$ , where  $D_{\text{diff}}$  is the diffusivity of the pertinent species. In this approximation, one uses the steady-state version of Eq. (9) on either side of the dividing surface but not *at* the dividing surface:

$$\nabla^2 \mu_i = 0, \quad r \gtrless R, \quad (36)$$

where we have assumed that  $\tilde{D}_{ij} = \tilde{D}_i \delta_{ij}$  and the diffusivities  $\tilde{D}_i$  are concentration-independent within each phase. The above equations are supplemented by the general boundary conditions, c.f. Eq. (12):

$$\begin{aligned} \mu_i(\mathbf{r} = \infty) &= 0 \\ \nabla \mu_i(\mathbf{r} = 0) &= 0. \end{aligned} \quad (37)$$

At the phase boundary, the following conditions must be obeyed:

$$\mu_i(R^-) = \mu_i(R^+) \quad (38)$$

$$\frac{1}{n_i^\ddagger} \left( \tilde{D}_i \frac{\partial \mu_i}{\partial r} \right) \Big|_{R^-}^{R^+} = \dot{R} \times \text{sign} \left[ n_i^{(\text{in},b)} - n_i^{(\text{out},b)} \right] \quad (39)$$

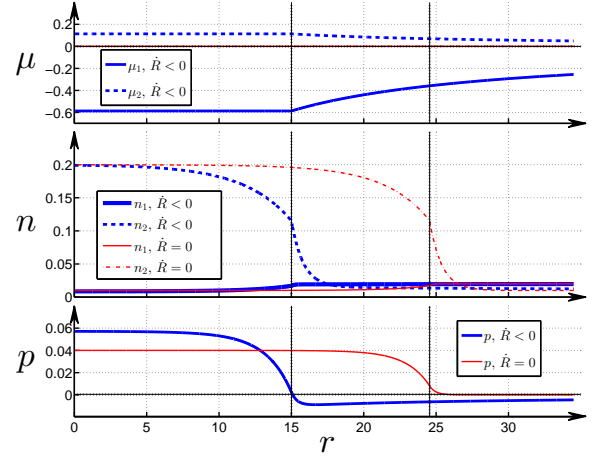


FIG. 4. The radial-coordinate dependences of the chemical potential  $\mu$ , concentrations  $n_i$ , and pressure  $p$  for a stationary ( $\dot{R} = 0$ , saddle-point) and non-stationary ( $\dot{R} < 0$ ) configuration of a spherical droplet. Note the chemical potentials in the stationary case  $\dot{R} = 0$  are equal to zero throughout:  $\mu_1 = \mu_2 = 0$ .

The chemical potential must be continuous to prevent uncompensated microscopic fluxes, hence Eq. (38). On the other hand, Eq. (39) ensures particle conservation at the boundary: An influx/outflow of the components at the phase boundary results in the growth or evaporation of the droplet. For instance, in a pure substance, the total particle influx,  $4\pi R^2 \tilde{D} (\partial \mu / \partial r)|_{R^-}^{R^+}$ , must be equal to  $4\pi R^2 n^\ddagger \dot{R}$  for a liquid droplet surrounded by vapor but will be equal to  $-4\pi R^2 n^\ddagger \dot{R}$  for a bubble of vapor surrounded by liquid. This is because a liquid droplet grows by collecting particles, while a bubble grows by *giving up* particles. The latter notion is reflected by the sign function in Eqs. (39). These equations, which apply to all  $M$  components, represent  $(M-1)$  constraints. The rate  $\dot{R}$  is deduced at the end of the calculation.

Eqs. (36), together with boundary conditions (37) and (38), imply that each chemical potential has the following functional form:

$$\mu_i = \begin{cases} \mu_i^\ddagger, & r \leq R \\ \mu_i^\ddagger(R/r), & r > R. \end{cases} \quad (40)$$

Thus compared with the original steady-state problem, there are  $M$  new unknown quantities  $\mu_i^\ddagger$  to be determined, while there are only  $(M-1)$  new constraints. This allows one to solve for the concentration profiles for values of the droplet radius  $R$  other than the stationary one.

To avoid confusion, we point out that in a non-stationary case, one must solve not the second-order equations (10) but the forth-order equations (9), at  $\dot{n}_i = 0$ . Thus, like the chemical potentials in Eq. (40), the concentration profiles will acquire  $1/r$  contributions (for  $r > R$ ) that reflect particle exchange with the bulk. Al-

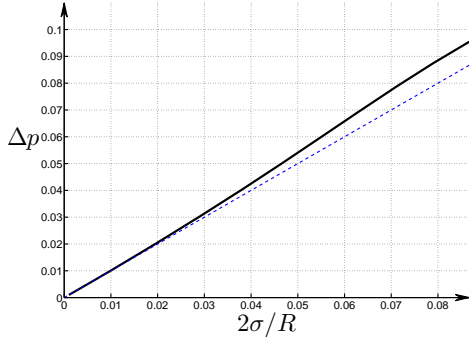


FIG. 5. The pressure difference  $\Delta p \equiv p(r=0) - p(r=\infty)$  plotted vs. the value  $2\sigma$  it would achieve in the thin interface limit, Eq. (26). Every point on both curves corresponds to a critical nucleus.

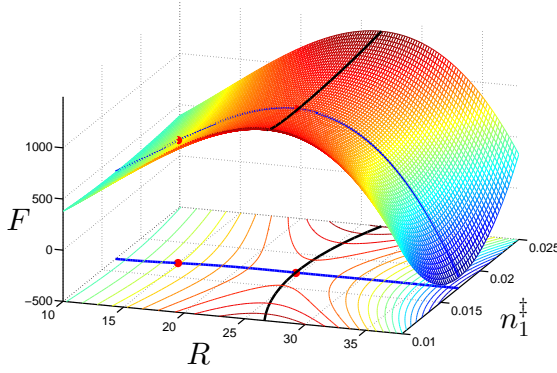


FIG. 6. The free energy surface of the droplet as a function of the radius  $R$  of the phase boundary and the concentration  $n_1^{\ddagger}$  of component 1. The dots indicate the two droplet configurations from Fig. 4. The line along the ridge of the surface corresponds to stationary points  $\dot{R} = 0$ ; of these points, only the lowest one is a true solution of Eq. (10). The other line is the steepest descent line for a droplet prepared at the saddle point.

though it involves solving transcendental equations for  $R$ , in view of Eqs. (34), the (numerical) solution of the problem (9) is straightforward and computationally robust. In Fig. 4, we graphically demonstrate such a solution for the binary mixture from Fig. 3 for both the stationary ( $\dot{R} = 0$ ,  $\mu_i = 0$ ) and a non-stationary case ( $\dot{R} < 0$ ,  $\mu_i \neq 0$ ). The corresponding  $(n_1, n_2)$  trajectories connecting the droplet center with the solution bulk are shown in Fig. 3. As remarked earlier, one expects that in steady state, the pressure is spatially uniform for a flat interface, while increasing monotonically toward the origin for a droplet with non-zero curvature. We observe in Fig. 4 that the converse is also true: For a non-critical droplet, the pressure no longer changes monotonically with the radial coordinate. In any event, the Laplace formula works reasonably well, despite the interface being thick, see Fig. 5.

In Fig. 6, we show the droplet free energy (4) as a function of  $R$  and  $n_1^{\ddagger}$ . In computing this free energy for non-stationary cases  $\dot{R} \neq 0$ , the  $1/r$  contributions were omitted. These contributions are associated with the bulk, not the droplet itself, and, appropriately, lead to divergent contributions to the free energy (4). As already discussed,  $(M-1)$  concentrations  $n_i^{\ddagger}$  are artificially not dynamical in the treatment because we do not explicitly solve Eqs. (10) at the phase boundary. This means that the  $\dot{R} = 0$  points form a  $(M-1)$ -dimensional surface in the  $(R, n_i^{\ddagger})$  space. When  $M = 2$ , this surface corresponds to a line; the latter line can be seen to run through a “ridge” on the  $F(R, n_1^{\ddagger})$  surface. The actual saddle point corresponds to the lowest point on the ridge. If prepared exactly on the ridge but away from the saddle point, the system will quickly relax to the saddle point. The characteristic time scale is given by  $R^2/\nu$ , where  $\nu \equiv \eta/\rho$  is the kinematic viscosity,  $\eta$  viscosity, and  $\rho$  mass density of the fluid. The kinematic viscosity, which has dimensions of the diffusivity, significantly exceeds the diffusivity itself at viscosities in question, i.e.,  $\eta > 10^{-2}$  Ps. This can be seen straightforwardly by comparing  $\eta/\rho$  and the Stokes-Einstein  $k_B T/(6\pi\eta a)$ , where  $a$  is a molecular size.

If prepared away from the ridge, the droplet will quickly relax along the  $n_i^{\ddagger}$  coordinates while also moving, relatively slowly, along the  $R$  coordinate. The latter evolution will lead to droplet growth or evaporation depending on which side of the ridge the system was initially prepared. The relaxation in the  $n_i^{\ddagger}$  coordinates corresponds to changes in the composition at the droplet interface. Such mixing processes involve hydrodynamic flows and are expected during phase ordering, as discussed early on by Siggia<sup>32</sup> and later, within a renormalization-group framework, by Bray.<sup>12</sup> While operating primarily along the phase boundaries for small volume fractions of the minority phase, such modes affect phase ripening when the latter volume fraction is sufficiently high. Last but not least, we note that according to Fig. 6, the chemical composition at the boundary depends only weakly on the droplet radius.

Note that the matching conditions (31) and (38) between the minority and majority phase are formally identical to those between phases that are in macroscopic equilibrium, as elucidated by Gibbs a long time ago. These matching conditions cover the chemical potentials of the individual species, pressure, and temperature. In the case of macroscopic coexistence, for each additional chemical species there could be, in principle, another phase in coexistence with those phases already present. In the present context, the number of phases is limited to two, by construction. The extra, “mixing” degrees of freedom stemming from increasing the number of components result in an increase of the dimensionality of the dividing surface in the  $\{n_i\}$  space, between the minority and majority phases.

## V. AMPHIPHILIC ADSORBENTS AT THE INTERFACE

We now consider a situation where no pressure “conservation” takes place. In mechanics, the energy is not conserved when the Lagrangian explicitly depends on time. Likewise, in the present problem, the full free energy density must explicitly depend on the coordinate:

$$\mathcal{V} = \mathcal{V}_n + \sum_i n_i \mathcal{V}_{\text{ext}}^{(i)}(\mathbf{r}), \quad (41)$$

where, by construction, the quantity  $\mathcal{V}_{\text{ext}}^{(i)}(\mathbf{r})$  is an external potential acting on species  $i$ ,  $\partial \mathcal{V}_{\text{ext}}^{(i)} / \partial n_j = 0$ , while  $\mathcal{V}_n$  does not explicitly depend on the coordinate:  $\partial \mathcal{V}_n / \partial \mathbf{r} = 0$ . More general forms of the coordinate-dependent portion of the full free energy density  $\mathcal{V}$  can be considered. For non-zero  $\mathcal{V}_{\text{ext}}^{(i)}(\mathbf{r})$ , Eqs. (6) can be written out as follows:

$$\begin{aligned} \sum_j \nabla(\kappa_{ij} \nabla n_j) - \frac{1}{2} \sum_{lm} \frac{\partial \kappa_{lm}}{\partial n_i} (\nabla n_l \nabla n_m) \\ = \frac{\partial \mathcal{V}_n}{\partial n_i} + \mathcal{V}_{\text{ext}}^{(i)}(\mathbf{r}) - \mu_i(\mathbf{r}), \end{aligned} \quad (42)$$

while Eq. (14) becomes

$$\begin{aligned} \sum_{ij} \frac{\kappa_{ij}}{2} \frac{dn_i}{dr} \frac{dn_j}{dr} \bigg|_1^2 - \mathcal{V}_n|_1^2 = -(D-1) \int_1^2 \frac{dr}{r} \sum_{ij} \kappa_{ij} \frac{dn_i}{dr} \frac{dn_j}{dr} \\ + \sum_i \int_1^2 dn_i [\mathcal{V}_{\text{ext}}^{(i)}(r) - \mu_i(r)], \end{aligned} \quad (43)$$

where a spherically-symmetric geometry is understood. Equations (21) through (23) can be rewritten for the specific form of the full free energy density from (41). And so for a flat interface,

$$p = -\mathcal{V}_n + \sum_{ij} \frac{\kappa_{ij}}{2} \frac{dn_i}{dx} \frac{dn_j}{dx} - \sum_i n_i [\mathcal{V}_{\text{ext}}^{(i)}(x) - \mu_i(x)]. \quad (44)$$

Thus, according to Eqs. (43) and (44), we conclude that the quantity on the l.h.s. of Eq. (43) does not correspond to a pressure difference, nor is it generally conserved in the presence of an external potential, even for a flat interface in complete equilibrium,  $\mu_i = 0$ .

Still, Eq. (44) implies that pressure changes continuously with the coordinate for a smooth external potential. In the spirit of the preceding Section, we next consider a *singular* potential so as to cause the pressure to experience a discontinuity. For the sake of argument, let us consider a flat interface in a one-component system. We choose the following form for the coordinate-dependent portion of the bulk free energy:

$$\mathcal{V}_{\text{ext}}(x) = -\epsilon \delta(x-L) + \epsilon \delta(x+L), \quad (45)$$

see sketch in Fig. 7(a). The above potential can be viewed as an extreme limit of a smoother potential that has an

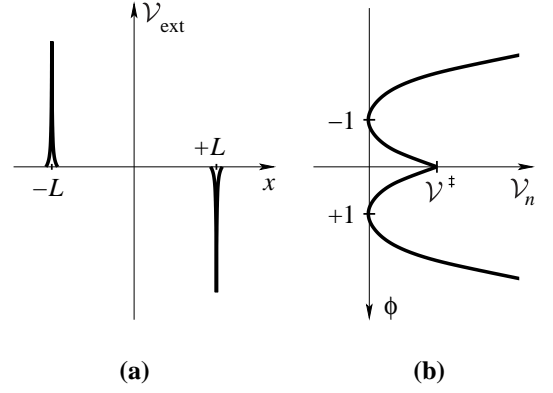


FIG. 7. **(a)** Schematic of the one-particle potential  $\mathcal{V}_{\text{ext}}$  from Eq. (45) for  $\epsilon > 0$ . **(b)** The concentration-dependent portion of the bulk free energy density  $\mathcal{V}_n$  from Eq. (41), employed in the present work to analyze the amphiphilic action. By Eq. (28),  $\mathcal{V}^\dagger = m/2$ .

attractive minimum centered at  $x = +L$  and a repulsive “hump” centered at  $x = -L$ .

By construction, the shapes of the attractive and repulsive parts are exactly the same; one may think of the potential in Eq. (45) as originating from a “dipole” of sorts. The latter potential can be thought of a stationary, externally-imposed field, but can be equally well thought of as resulting from adding an amphiphilic species—or detergent—to the system. Indeed, suppose we are not concerned with the total density in a binary solution but only with the *partial* quantity of the components. The partial quantity can be described using a single order parameter  $\phi$ . This way, the derivative  $\partial \mathcal{V} / \partial \phi$  is related to the actual chemical potentials of the components in a linear fashion. For convenience, one may choose the minima of the free energy density  $\mathcal{V}$  to be at  $\phi = \pm 1$ , see Fig. 7(b). The potential (45) can be thought of as a field acting on linear molecules so that their two tails prefer to stay in the phases that are relatively rich in the two components of the mixture respectively. Specifically, for the bulk free energy density in Fig. 7(b), the l.h.s. and r.h.s. peaks of  $\mathcal{V}_{\text{ext}}$  in Fig. 7(a) serve as a repulsive bump and attractive minimum, respectively, in the  $\phi > 0$  phase. The situation is reversed in the  $\phi < 0$  phase. The quantity  $\epsilon$ , by construction, reflects the surface concentration of the amphiphiles but also their solvation free energy. We will call the quantity  $\epsilon$  the *activity* for brevity. To avoid confusion we note that this is *not* the standard definition of the activity of a component in a solution. (Note the quantity  $\epsilon$  could have either sign.)

What are the appropriate boundary conditions for a singular potential of the type from Eq. (45)? A definitive answer to this question can be obtained, if the coefficient  $\kappa$  is a continuous function of the concentration near  $x = \pm L$ . (The situation to the contrary will be discussed shortly.) Because the potential  $\mathcal{V}_{\text{ext}}$  is infinitely narrow,  $\kappa$  can be regarded as a constant on the lengthscale of the spatial variation of  $\mathcal{V}_{\text{ext}}$ . In the mechanics analogy,



we now have a situation where the *energy* is no longer conserved: Each  $\delta$ -function peak in Eq. (45) corresponds to an infinitely rapid “kick.” The resulting increment in the momentum is given by the time integral of the kick, by Newton’s third law. This notion can be implemented in the present context by integrating Eq. (42) in terms of  $x$  from  $L^-$  to  $L^+$  (and likewise for the l.h.s. peak from Eq. (45)). One gets, as a result:

$$\kappa \frac{d\phi}{dx} \Big|_{\pm L^-}^{\pm L^+} = \mp \epsilon. \quad (46)$$

Note that using Eq. (43) would *not* yield unambiguous boundary conditions because computing the integral  $\int d\phi \mathcal{V}_{\text{ext}} = \int dx (d\phi/dx) \mathcal{V}_{\text{ext}}$  requires the knowledge of the derivative  $d\phi/dx$  *exactly* at the point of singularity. However, the quantity  $d\phi/dx$  experiences a discontinuity at the singularity and thus is not well-defined there. Incidentally, we point out that a problem in which a  $\delta$ -function-like potential is placed exactly at the phase boundary is generally ill-defined mathematically in the sense that one cannot place a constraint on the concentration gradient of the type from Eq. (31) or (46). To appreciate this, one may invoke the mechanics analogy once again and think of the singularities in the bulk free energy density  $\mathcal{V}_n$  and the one-particle potential  $\mathcal{V}_{\text{ext}}$  not as confined to an infinitely narrow region of the coordinate and time respectively, but, instead, as smeared over *finite* ranges of the respective variables. At the same time, the values of the momenta specified on the two sides of the original singularity should be now thought of as specified at infinity. Presented in this form, the setup of the problem is entirely analogous to how one thinks of scattering events. In one-dimensional space, one can evaluate the particle’s momentum long after such a scattering event without having to solve detailed equations of motion at intermediate times, if either energy or momentum are conserved (or both), but not otherwise. We thus conclude that a limit when a discontinuity in  $\mathcal{V}$  or its derivative and a  $\delta$ -function-like potential  $\mathcal{V}_{\text{ext}}$  exactly coincide in space, is ill-defined. This is not a real issue in practice, since the distance (coordinate-wise) between the two singularities can be made arbitrarily small; we shall see this shortly.

To illustrate the above discussion we find the density profile for a flat interface in the presence of external potential (45), subject to boundary conditions:

$$\phi(+\infty) = 1 \quad (47)$$

$$\phi(-\infty) = -1. \quad (48)$$

For clarity, we assume  $\kappa = \text{const.}$  It is obvious from the symmetry of the problem that the optimal position of the phase boundary  $x_{\text{int}}$ , defined as  $\phi(x_{\text{int}}) = 0$ , is exactly at the origin. (The subscript “int” refers to “interface.”) The origin, we remind, is at the midpoint of the “dipole”-like potential in Eq. (45) by construction. This notion can be made even more explicit by plotting

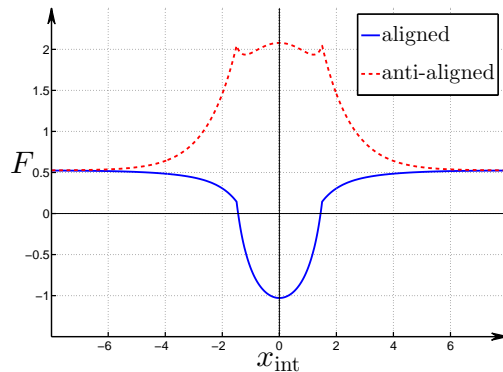


FIG. 8. The free energy of the interface in the presence of potential  $\mathcal{V}_{\text{ext}}$  from Eq. (45), plotted as a function of the distance  $x_{\text{int}}$  between the phase boundary and the midpoint of the potential. Here,  $L = 1.5$ ,  $\epsilon = +1$  bottom term,  $\epsilon = -1$  top term.

the free energy of the system as a function of  $x_{\text{int}}$ . Since  $x_{\text{int}} \neq 0$  configurations are non-stationary, we must solve the full problem (9) under such circumstances. As in the preceding Section, we instead solve a steady-state problem in which  $\nabla^2 \mu = 0$  is everywhere except at  $x = \pm L$  and the phase boundary. In 1D, this equation is solved by a linear function, leaving us with the following option, up to an additive constant:

$$\mu(x) = \begin{cases} 0, & x < x_1, x_3 \leq x \\ \mu_0(x - x_1)/(x_2 - x_1), & x_1 \leq x < x_2 \\ \mu_0(x_3 - x)/(x_3 - x_2), & x_2 \leq x < x_3, \end{cases} \quad (49)$$

where  $x_1$ ,  $x_2$ , and  $x_3$  ( $x_1 < x_2 < x_3$ ) are assigned to the locations of the three singularities in the ascending order. The presence of the sloped portion of the chemical potential in Eq. (49) reflects that away from equilibrium, the material must be exchanged within the  $(x_1, x_3)$  interval—but not between the bulk phases!—in order to relax toward equilibrium. The appearance of a new unknown  $\mu_0$  allows us to regard the distance  $x_{\text{int}}$  as a free parameter. The resulting interface free energy per unit area, as a function of  $x_{\text{int}}$ , is shown in Fig. 8. In this Figure, we show the free energy in two specific situations, where the pinning potential is “aligned” with the boundary conditions (47)-(48),  $\epsilon > 0$ , and anti-aligned  $\epsilon < 0$ , respectively. While the attractive minimum and overall repulsion near  $x_{\text{int}} = 0$  for the aligned and anti-aligned configurations respectively are expected, it is less obvious that there should be some structure to the repulsive maximum in the upper term. Here and in the rest of the Section, we use units such that the length  $\sqrt{\kappa/m}$  and the surface tension coefficient of a standalone interface, which is  $\sqrt{\kappa m}$  by Eq. (27), are both set to unity.

We now illustrate two specific configurations of the interface for  $x_{\text{int}} \neq 0$ , pertaining to the bottom term in Fig. 8. These configurations correspond to two distinct mutual arrangements of the phase boundary and the po-

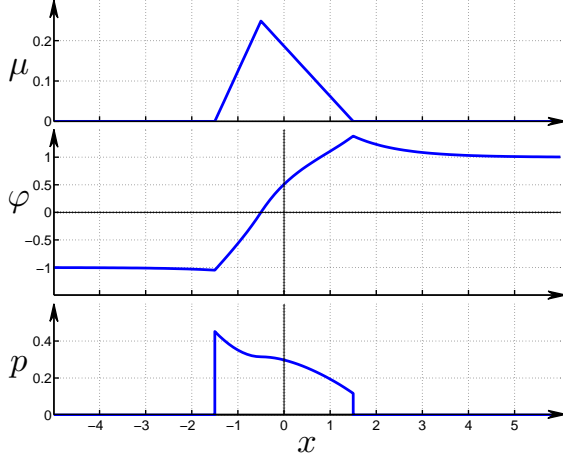


FIG. 9. The coordinate dependences of the chemical potential  $\mu$ , order parameter  $\phi$ , and pressure  $p$  for a specific configuration corresponding to  $x_{\text{int}} = -0.5$  of the bottom (bonding), term from Fig. 8.  $L = 1.5$ . Hereby, the phase boundary is located between the peaks of the potential  $\mathcal{V}_{\text{ext}}$  from Eq. (45). The  $\delta$ -function contributions to pressure are not shown.  $\epsilon = 1$ .

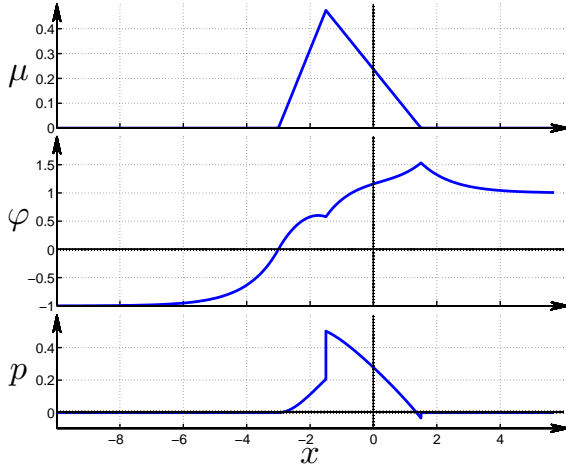


FIG. 10. The coordinate dependences of the chemical potential  $\mu$ , order parameter  $\phi$ , and pressure  $p$  for a specific configuration corresponding to  $x_{\text{int}} = -3$  of the bottom (bonding), term from Fig. 8.  $L = 1.5$ . The phase boundary is to the left of both peaks of the potential  $\mathcal{V}_{\text{ext}}$  from Eq. (45), c.f. Fig. 9.  $\epsilon = 1$ .

tential, see Figs. 9 and 10, where the phase boundary is located, respectively, between the singularities of the pinning potential  $\mathcal{V}_{\text{ext}}$  and outside (to the left of) those singularities.

Note that in the symmetric cases,  $x_{\text{int}} = 0$  (not shown), which are both optima of the free energy, the chemical potential is zero throughout. Under these circumstances, the pressure is now a conserved quantity and thus must be uniform in the  $-L < x < L$  interval, by Eqs. (24). (Recall, the potential  $\mathcal{V}_{\text{ext}}$  is zero in that interval.) Within the  $-L < x < L$  interval, the pressure

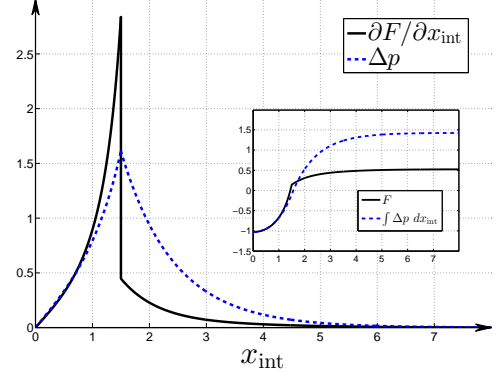


FIG. 11. Solid line: The coordinate derivative of the free energy of the interface in the presence of potential  $\mathcal{V}_{\text{ext}}$  from Eq. (45), plotted as a function of the distance  $x_{\text{int}}$  between the phase boundary and the midpoint of the potential. Dashed line: Difference between the pressure discontinuities at the ends of the amphiphile, also as a function of  $x_{\text{int}}$ .

is positive and negative for the aligned and anti-aligned configurations, respectively.

It is interesting to ask how big a portion of the free energy  $F(x_{\text{int}})$  in Fig. 8 accounts for the work needed to move the amphiphile; the remainder is used to redistribute the liquid itself. In answering this question, we show in Fig. 11 the derivative of the free energy  $F(x_{\text{int}})$  with respect to the location  $x_{\text{int}}$  and the difference between the pressure discontinuities at points  $x = \pm L$ , both as functions of  $x_{\text{int}}$ . The integrals of both quantities w.r.t. to the coordinate are shown in the inset. One observes that the mechanical work expended in bringing the amphiphile from the bulk is substantially offset by the free energy cost of redistribution of the solvent near the amphiphile.

The rest of the Section focuses exclusively on the equilibrium configuration, which corresponds to the minimum in the bottom, “bonding” term in Fig. 8, located at  $x_{\text{int}} = 0$ . Of greatest interest is the degree of renormalization of the surface tension as a function of the activity  $\epsilon$  of the amphiphile, which is illustrated in Fig. 12, for three specific values of the amphiphile half-length  $L$ . Note that for any value of  $L$ , there are critical values of the activity beyond which the interface tension is exactly compensated by the “solvation” energy of the amphiphile leading to a vanishing of the effective surface tension. This can be seen explicitly in Fig. 12. We note that for sufficiently large and *negative* values of  $\epsilon$ , the curves in Fig. 12 bend down and cross the origin. This is because in the (somewhat trivial) limit  $\epsilon \rightarrow \pm\infty$ , the intrinsic energy scale of the interface becomes negligible and the response of the heterophase system can be approximated by that of a pure phase.

The value of the surface tension  $\sigma$  cannot be negative, of course. As  $\sigma$  becomes sufficiently small—but still positive—several things could happen after more am-

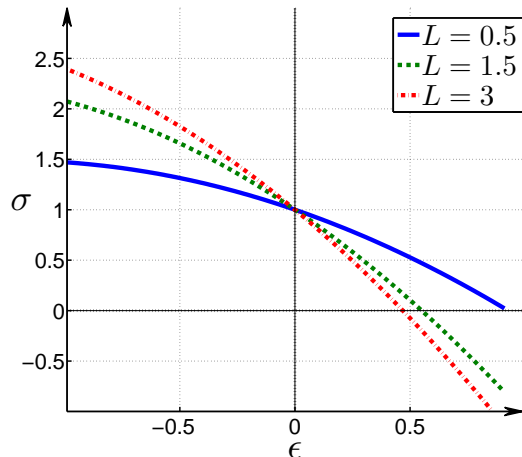


FIG. 12. Dependence of the free energy of the interface on the activity  $\epsilon$  of the amphiphile, for three distinct values of  $L$ . All curves correspond to the stable minimum in Fig. 8,  $x_{\text{int}} = 0$ , bottom term.

phiphile is added to the solution, depending on circumstances. If the interface is not allowed to break up into smaller pieces, it will spontaneously begin to distort so as to increase in area and become able to accommodate additional detergent. This is a realization of the Krafft point.<sup>33</sup> The distortion of the interface will occur at a *positive* value of  $\sigma$ , even if relatively small, because of the non-zero vibrational entropy of the interface. On the other hand, if equilibrated—which could be facilitated by stirring—the system can lower its free energy by breaking the original interface into smaller pieces thus leading to the formation of a *suspension* of the minority phase covered with the detergent. This is, of course, how soap works.

## VI. INTERFACE WETTING IN GLASSY LIQUIDS

As already remarked, the potential (45) can be viewed either as that due to an amphiphilic molecule or, equally well, as an externally imposed potential. This potential pins the interface, Fig. 8, but also down-renormalizes its tension, Fig. 12. Down-renormalization of the surface tension is of central significance in the random field Ising model<sup>34</sup> (RFIM) and in the context of the free energy landscape and activated transport in glassy liquids.<sup>19,24</sup> In contrast with conventional phases of matter, as originally envisioned by Gibbs, glassy liquids are characterized by a complex free energy landscape, where the number of free energy minima scales exponentially with the system size  $N$ :  $e^{s_c N}$ , where  $s_c$  is the configurational entropy per particle.<sup>20,35,36</sup> This multiplicity of minima reveals itself directly as the excess liquid entropy relative to the corresponding crystal. According to the random first

order transition (RFOT) theory,<sup>19</sup> liquid transport is realized via activated transitions between the free energy minima. The minima are deep enough that the lifetime of the structures corresponding to each minimum greatly exceeds the vibrational time. The activated transport on the landscape proceeds via nucleation-like events; the free energy cost for reconfiguring a compact region of size  $N$  reads:

$$F(N) = -T s_c N + \gamma \sqrt{N}. \quad (50)$$

The bulk-driving force for reconfiguration ( $-T s_c N$ ) is due to the exponential multiplicity of free energy minima. The surface tension portion  $\gamma \sqrt{N}$  scales with the droplet radius  $R \propto N^{1/D}$  as  $R^{D/2}$ , not the conventional  $R^{D-1}$ . This corresponds to an effective surface tension coefficient that decreases with the radius as  $R^{D/2}/R^{D-1} = R^{1-D/2}$  and thus vanishes for macroscopic interfaces in any number of spatial dimensions higher than  $D = 2$ . A detailed argument<sup>34,36,37</sup> shows that this renormalization can be thought of as resulting from a distortion of the original, relatively thin interface so as to locally optimize free energy.<sup>36</sup> The latter fluctuations are transiently frozen-in and obey the usual Gaussian statistics. The down-renormalization of the mismatch penalty results in a lowering of the barrier for activated transport. Quantitative estimates<sup>20,23,37-39</sup> for the barrier are in good agreement with observation, without using adjustable parameters. As a result of the distortions, the interface becomes fractal in shape, with an effective width scaling with the droplet radius itself. An analogy between free energy fluctuations in a glassy liquid and the random on-site field of the random-field Ising model (RFIM) was originally pointed out and exploited by Kirkpatrick, Thirumalai, and Wolynes,<sup>36</sup> while a procedure to map a specific liquid-model onto the RFIM has been developed by Stevenson et al.<sup>40</sup>

In a related picture put forth by Bouchaud and Biroli,<sup>41</sup> each long-lived compact structure can be thought of as fitting its environment better than a generic aperiodic arrangement of particles within the corresponding region. Hereby, the partition function of the region, with a fixed environment (up to vibration), consists of two contributions: that of an essentially unique contribution of the well-fitting structure and that of the rest of the configurations:

$$Z(N) = e^{-\beta(-\gamma N^x)} + e^{s_c N}. \quad (51)$$

In the Bouchaud-Biroli (BB) argument, the exponent  $x$  at the stabilization free energy ( $-\gamma N^x$ ) is not specified, except that it must be less than one. The argument is agnostic as to the detailed mechanism of escape from the long-lived state.

The pictures leading to Eqs. (50) and (51) are complementary<sup>42</sup> and can be thought of as differing with regard to the free energy reference. The former picture starts from a stabilized state and considers the free energy cost of escaping from such a stable state, which is incurred

because two randomly chosen distinct structures do not mutually fit. In the BB picture, one starts from a high free energy state as resulting from bringing in contact two dissimilar structures; the strain is uniformly high in such a state. One then picks through alternative structures within a compact region of some size  $N$  until the best match is found that lowers the free energy to the greatest extent. The two pictures lead to the same size  $N^*$  of the cooperatively rearranging region:

$$\gamma\sqrt{N^*} = T s_c N^*, \quad (52)$$

while the exponent  $x$  from Eq. (51) may be fixed at  $1/2$ , see a detailed discussion by Lubchenko and Rabochiy<sup>37</sup> (and also a recent review<sup>24</sup>). The latter authors have argued the term  $\gamma\sqrt{N}$  can be thought of as the magnitude of a typical fluctuation of the Gibbs free energy at size  $N$ . Consistent with the large breadth of the distorted interface, the mismatch penalty between the region and its environment is distributed over the whole region, in contrast with the DFT-based picture from Section IV, in which the penalty is accrued largely over a narrow shell.

In the context of the preceding Section, one may view the random field of the RFIM (and, hence, the frozen-in fluctuations of the RFOT) as a collection of stationed amphiphilic molecules that are distributed uniformly in space. The molecules are randomly oriented and sized. Indeed, because the on-site field is zero on average, for each site with a field oriented in a particular direction, there will be a site with a field equal in magnitude and opposite in direction.

It is easy to see that beyond a certain threshold value of the magnitude of the on-site field, an originally smooth interface will distort spontaneously. As discussed in Section V, if the activity of the amphiphile exceeds a certain value, the total amount of interfacial regions begins to increase. This results either in a bigger number of droplets or in a distortion of the interface, if the number of droplets cannot change for some reason. (The two options are not as distinct as one might think, see below.) Suppose we start with a relatively thin interface confined to a region of size  $N$  particles; the interface separates two dissimilar aperiodic structures. We thus set our reference state in the Bouchaud-Biroli way. In the presence of the “amphiphiles,” the boundary will distort some. Since the amphiphiles are distributed uniformly in space, the interface will come in contact with a new set of the amphiphiles and distort some more. The interface will continue distorting until the interfacial material covers all the amphiphiles contained within the region.

One can view the distorted interface as having the same *bare* surface tension coefficient as a standalone undistorted interface but stretched and covering more amphiphiles, see Fig. 13(a). In this view, the decreased *effective* surface tension is due to the solvation energy of the amphiphiles that are in contact with the interface, despite the greatly increased area of the distorted interface. The distortion takes place in a continuous range of wavelengths. The process of distortion can be broken

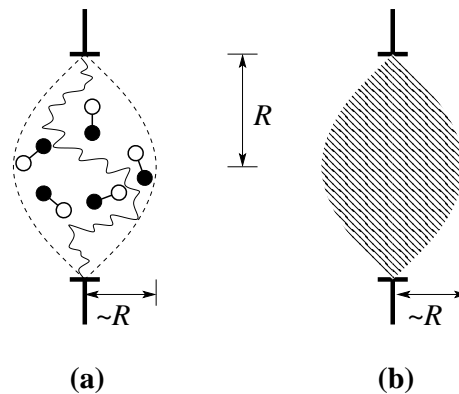


FIG. 13. (a) Cartoon depicting a distorted interface subjected to uniformly seeded amphiphilic molecules. (b) A renormalized view of panel (a), in which the amphiphiles are effectively accounted for through a thicker, softened interface.

up into a sequence of elemental steps, each of which occurs in a narrow wavelength range  $[r, r + dr]$ .<sup>24,34,36,37</sup> This sequence constitutes a continuous renormalization-group transformation. The end result of this transformation, up to wavelength  $R$ , is an effective interface that is not stretched but is thicker and *softer*, see sketch in Fig. 13(b). The renormalized interface covers fewer amphiphiles, because some of the amphiphiles are already effectively accounted for through the softened tension. The renormalization-group argument is standard;<sup>34,36</sup> it was revisited recently<sup>37</sup> and will not be repeated here. The role of the on-site field is now played by the local value of the amphiphile activity  $\epsilon$ . Lubchenko and Rabochiy<sup>37</sup> used an RG line of thought to argue that given a sufficiently large value of  $R$ , surface renormalization occurs for any positive value of  $\epsilon$ , no matter how small. The basic reason is that the stabilization due to the distortion scales as  $\epsilon(\delta N)^{1/2}$ , where  $\delta N$  is the number of amphiphiles “swept” during an individual step in the renormalization procedure. The penalty for stretching of the interface scales with a higher power of  $\delta N$  and thus always inferior to  $\sqrt{\delta N}$  at sufficiently small  $\delta N$ , so long as  $\epsilon > 0$ .<sup>37</sup>

The scaling of the eventual amount of renormalization with the region size can be deduced with little effort by noting that the extent of renormalization scales approximately linearly with the total activity of the amphiphilic molecules residing within the boundary, see Fig. 12. Since the orientations of the latter molecules are random, the total activity is on average zero, but could be either positive or negative for a specific configuration of the interface. The magnitude of such total activity fluctuation scales as the usual  $\sqrt{N}$ , by the law of large numbers. The latter law applies when the correlation length  $\sqrt{\kappa/m}$  is not too large, which is indeed the case.<sup>23</sup> Negative fluctuations will be more likely than the positive ones, according to Boltzmann. These negative fluctuations will lead to a stabilization of the region in question, the amount of stabilization scaling as  $\sqrt{N}$ , as



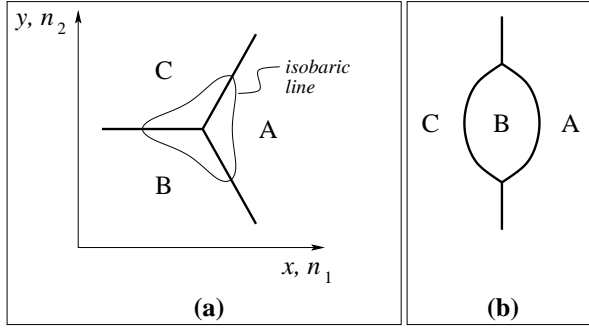


FIG. 14. (a) Three co-existing phases A, B, and C in contact. The horizontal axis denotes both the Cartesian axis  $x$  and, roughly, the direction of the  $\nabla n_1$  gradient. Likewise, the vertical axis denotes both the Cartesian axis  $y$  and the direction of the  $\nabla n_2$  gradient. In this arrangement, isobaric lines are not too different from the  $\mathcal{V} = \text{const}$  lines, by Eq. (21). (b) A droplet of phase B sandwiched between phases A and C. Regions of three-phase coexistence can be approximated as in the (a) panel.

just said. The latter stabilization corresponds with the  $-\gamma N^x$  term in Eq. (51), at  $x = 1/2$ , and is consistent with the picture advanced by the RFOT theory.

As follows from the above discussion, a macroscopically large flat interface will continue to distort indefinitely, in the presence of uniformly seeded amphiphiles ( $R \rightarrow \infty$  limit in Fig 13). This is why the effective surface tension coefficient of a flat interface *vanishes* in the RFOT theory. One may say that there is no conventional surface tension between alternative aperiodic minima of free energy in glassy liquids, in the sense of the classical nucleation theory. It turns out that the main formula of this article, Eq. (21), provides an additional perspective on this fascinating fact, if combined with earlier ideas of Xia and Wolynes.<sup>20</sup> The latter authors pictured the surface tension renormalization as a “wetting” of the interface between two distinct meanfield free energy minima of the glassy liquid by configurations that are representative of *other* meanfield minima.<sup>20</sup>

In considering interface wetting, let us use a bulk free energy density that does not explicitly depend on the coordinate:  $\partial \mathcal{V} / \partial \mathbf{r} = 0$ . To set the stage, we first consider the geometry in which three nearly flat, intersecting interfaces separate some three distinct liquid phases, call them A, B, and C. The three interfaces intersect along the same straight line, see Fig. 14(a). This geometry can also be thought of as approximating a small portion of an oblate bubble of phase B residing between two distinct phases A and C, see Fig. 14(b). Formally, to realize such a three-phase fluid coexistence, the liquid must consist of at least two components, by the Gibbs phase rule. By construction—and for future convenience—suppose phase A is relatively rich in component 1 and intermediate with regard to the content of component 2. Phase B is poor in both components, and C is poor in component 1 and rich in component 2, see Fig. 14(a). The isobaric

surfaces are roughly similar to the  $\mathcal{V} = \text{const}$  surfaces, but certainly not to the  $n_i = \text{const}$  surfaces. The former surfaces are represented by closed contours centered generically at the three-phase boundary. The  $n_i = \text{const}$  surfaces, in contrast, are approximately parallel to the  $x$  and  $y$  axes on Fig. 14(a).

Because the external normal to an isobaric surface is no longer collinear with the concentration gradients, the first term under the sum in Eq. (21) is significantly reduced compared with a spherically symmetric situation, much more so than the second term. This is particularly obvious if one sets the off-diagonal elements  $\kappa_{ij}$ ,  $i \neq j$  to zero. (A quick thought shows that the contribution of the off-diagonal terms in the geometry from Fig. 14(a) is relatively small even if the off-diagonal  $\kappa_{ij}$  are non-zero, because the  $\nabla n_i$  gradients are mutually, approximately orthogonal.) To estimate the reduction in the first term, assume the gradients of each concentration  $n_i$  preserve their directions as one goes around an isobaric surface. Meanwhile, the external normal  $\mathbf{e}$  performs a full rotation per each closed path around the line. Under these circumstances, the average  $\langle (\mathbf{e} \nabla n_i) (\mathbf{e} \nabla n_j) \rangle \simeq (1/D) \langle (\nabla n_i \nabla n_j) \rangle$  in  $D$  spatial dimensions. Indeed, the rotational average  $\langle e_i e_j \rangle = \delta_{ij} (1/D)$ , where  $e_i$  is the  $i$ -th component of the unit vector  $\mathbf{e}$ . This is because  $\langle e_i e_j \rangle \propto \delta_{ij}$  and  $\sum_i e_i e_i = 1$ .

We thus observe that in the geometry of Fig. 14(a),  $D = 2$ , the two terms under the sum in Eq. (21) largely compensate each other. The latter equation thus yields that the region in which the three phases coexist is at *negative* pressure, relative to the bulk. This is expected and constitutes a mechanically-stable geometry: The line where the three phases meet can be thought of as being suspended and pulled on by the two-phase boundaries. Likewise, a point in 3D space where four distinct liquid phases meet, would be suspended on the lower-order phase boundaries and would be even at yet lower pressure, since the first term under the sum in Eq. (21) would get only smaller with  $D$ .

Imagine now a spherical droplet of one phase surrounded by another phase and suppose that the boundary is wetted by a large number of alternative phases similarly to how the A-C interface is wetted by phase B in Fig. 14(b). Imagine that new interfaces appearing during wetting are further wetted and so on, down to the correlation lengthscale  $\sqrt{\kappa/m}$  of the Landau-Ginzburg theory for an individual phase. According to the above argument, the pressure must *decrease* as one moves inward from the bulk toward the center of the droplet. Now, because there are no phase boundaries to suspend the low pressure region on, the latter region would *collapse*. Alternatively, this situation could be thought of a corresponding to a negative surface tension coefficient, by Eqs. (25) and (26). At their face value, the above notions are simply a consequence of the Gibbs rule: Given a finite number of components, only a finite number of phases is allowed and so the unlimited wetting described above is impossible.

Yet in glassy liquids, the number of possible “phases,” which correspond with distinct free energy minima, grows exponentially with volume and is thus effectively unlimited. Hence we conclude that the mismatch penalty between distinct free energy minima in a glassy liquid cannot be defined in the conventional way. This notion is consistent with our earlier discussion of the surface tension renormalization in the presence of a random field, but it also fleshes out the “wetting” perspective on the renormalization of the mismatch penalty.

In applying the present result to glassy liquids, an important caveat must be made. Strictly speaking, the functional (4) applies to *fluids*, in which the shear modulus is zero. In arriving at Eq. (50), one adopts the view that the “minority phase” is an equilibrated liquid, by construction. The environment, on the other hand, represents a mechanically stable (aperiodic) solid, on the pertinent timescale. A solid can, in fact, support a compact region of negative pressure. This notion does not invalidate the present analysis so long as the glassy liquid is equilibrated on the laboratory timescale and so the reconstructions occur without a volume change. Still, there may be some residual stresses in the environment due to local inhomogeneity in stress. Such inhomogeneities would be present even in a periodic crystal, let alone an aperiodic one.<sup>43–45</sup> Already the spatially-inhomogeneous bulk free energy from Eq. (41) captures, in part, long-range correlations that may arise as a result. Indeed, the field from an elastic “dipole” made of two point-like forces can be emulated using the free energy functional (4) by making the coefficients  $m_{ij}$  from Eq. (28) sufficiently small. A full treatment, however, must include off-diagonal entries of the strain-tensor. Such treatments are available at the strict mean-field<sup>46</sup> and higher, Onsager-cavity<sup>47</sup> levels.

## VII. SUMMARY

This work analyzes several phenomena in the area of phase transitions from a *mechanical* vantage point. It takes advantage of a formal analogy between the Lagrangian formalism in classical mechanics and the Landau-Ginzburg description of macroscopic phase coexistence, in which the analog of time is the spatial coordinate that traverses the phase boundary. Pressure, which is the partial derivative of the free energy with respect to that spatial coordinate, is formally analogous to the mechanical energy, which is the partial derivative of the action with respect to time. This analogy allows one to generalize the old—and surprisingly little known—results of van der Waals on phase coexistence to multi-component mixtures and certain off-equilibrium situations. While automatically yielding that Pascal’s law must be obeyed during macroscopic coexistence, the approach can be extended straightforwardly to spherical geometries of the minority phase and, in some cases, to other geometries. The so obtained mechanical perspec-

tive on phase coexistence allows one to make progress in several problems that are seemingly disparate yet turn out to be connected.

In the first problem, of interest to mesoscopic phases in liquid solutions, we establish that certain singular forms of the bulk free energy density are amenable to essentially analytical solution in individual phases. To patch the solutions at the phase boundary, where the bulk free energy density is singular, one must require that pressure be a continuous function of the coordinate. We straightforwardly obtain a saddle-like free energy profile for a nucleus of the minority phase. The coordinate transverse to the nucleus size corresponds to the chemical composition at the interface. The coordinate is interesting in that its dynamics do not involve particle exchange with the bulk; it thus must operate along the phase boundary, consistent with earlier, hydrodynamics-based analysis by Siggia.<sup>12,32</sup> The chemical composition at the interface is seen to depend only weakly on the droplet radius.

The opposite situation of the *violation* of Pascal’s law leads us to a model that has a double use: Surface tension renormalization in the presence of a pinning potential or in the presence of amphiphiles. Simple relations between the amount of renormalization and the activity of the amphiphile are established.

In the two setups above, Pascal’s law is obeyed and violated respectively. Although seemingly distinct, the two situations turn out to be two faces of the same coin in the final problem analyzed in this work. Here we argue that the complicated problem of down-renormalization of the mismatch penalty between alternative aperiodic structures in glassy liquids can be thought about in a relatively simple fashion: On the one hand, the renormalization can be viewed as a distortion of the interface separating two dissimilar structures in the presence of uniformly seeded, randomly oriented amphiphiles. On the other hand, the renormalization of the mismatch can be viewed as extensive wetting of the interface by yet other aperiodic structures. In both views, Pascal’s law is violated, yet in the latter view, it is violated only transiently since the bulk free energy does not explicitly depend on the coordinate. This reflects that the disorder in glassy liquids is self-generated, not quenched. Both views indicate that the mismatch between alternative structures cannot be described using conventional notions of the density functional theory even in the thick interface limit. Yet the amphiphile view, which is rooted in those same notions, allows a way out of this seeming impasse: The renormalization can be thought of an essentially bulk effect due to a random field (as stemming from the amphiphiles), which is zero on average. When it happens to be non-zero in any specific region, this field scales at most as the square root of the region size, thus resulting in a square root scaling of the mismatch penalty with the region size. This scaling is consistent with the RFOT theory.

*Acknowledgment.* The authors thank Peter G. Wolynes and Peter G. Vekilov for inspiring conversations. They gratefully acknowledge support by the National Sci-

ence Foundation (MCB-1244568, CHE-0956127) and the

Welch Foundation Grant E-1765.

- 
- \* vas@uh.edu
- <sup>1</sup> L. D. Landau and E. M. Lifshitz, *Statistical Mechanics* (Pergamon Press, New York, 1980).
  - <sup>2</sup> R. S. Berry, S. A. Rice, and J. Ross, *Physical Chemistry* (John Wiley & Sons, Hoboken, NJ, 1980).
  - <sup>3</sup> J. S. Rowlinson and B. Widom, *Molecular Theory of Capillarity* (Clarendon Press, Oxford, 1982).
  - <sup>4</sup> J. van der Waals, *J. Stat. Phys.* **20**, 200 (1979).
  - <sup>5</sup> J. Rowlinson, *J. Stat. Phys.* **20**, 197 (1979).
  - <sup>6</sup> H. W. Cahn and J. E. Hilliard, *J. Chem. Phys.* **28**, 258 (1958).
  - <sup>7</sup> J. W. Cahn, *J. Chem. Phys.* **30**, 1121 (1959).
  - <sup>8</sup> J. W. Cahn and J. E. Hilliard, *J. Chem. Phys.* **31**, 688 (1959).
  - <sup>9</sup> E. W. Hart, *Phys. Rev.* **113**, 412 (1959).
  - <sup>10</sup> J. G. Kirkwood and F. P. Buff, *J. Chem. Phys.* **17**, 338 (1949).
  - <sup>11</sup> R. Evans, *Adv. Phys.* **28**, 143 (1979).
  - <sup>12</sup> A. J. Bray, *Adv. Phys.* **43**, 357 (1994).
  - <sup>13</sup> O. Gliko, N. Neumaier, W. Pan, I. Haase, M. Fischer, A. Bacher, S. Weinkauff, and P. G. Vekilov, *JACS* **127**, 3433 (2005).
  - <sup>14</sup> Y. Georgalis, P. Umbach, W. Saenger, B. Ihmels, and D. M. Soumpasis, *J. Amer. Chem. Soc.* **121**, 1627 (1999).
  - <sup>15</sup> O. Gliko, W. Pan, P. Katsonis, N. Neumaier, O. Galkin, S. Weinkauff, and P. G. Vekilov, *J. Phys. Chem. B* **111**, 3106 (2007).
  - <sup>16</sup> W. Pan, P. G. Vekilov, and V. Lubchenko, *J. Phys. Chem. B* **114**, 7620 (2010).
  - <sup>17</sup> J. S. Langer, *Rep. Prog. Phys.* **77**, 042501 (2014).
  - <sup>18</sup> G. Biroli and J. P. Garrahan, *J. Chem. Phys.* **138**, 12A301 (2013).
  - <sup>19</sup> V. Lubchenko and P. G. Wolynes, *Annu. Rev. Phys. Chem.* **58**, 235 (2007).
  - <sup>20</sup> X. Xia and P. G. Wolynes, *Proc. Natl. Acad. Sci. U. S. A.* **97**, 2990 (2000).
  - <sup>21</sup> D. M. McQuarrie, *Statistical Mechanics* (Harper-Collins, New York, 1973).
  - <sup>22</sup> L. D. Landau and E. M. Lifshitz, *Theory of Elasticity* (Pergamon Press, 1986).
  - <sup>23</sup> P. Rabochiy and V. Lubchenko, *J. Chem. Phys.* **138**, 12A534 (2013).
  - <sup>24</sup> V. Lubchenko, *Adv. Phys.* **64**, 283 (2015).
  - <sup>25</sup> L. Onsager, *Phys. Rev.* **37**, 405 (1931).
  - <sup>26</sup> L. Onsager, *Phys. Rev.* **38**, 2265 (1931).
  - <sup>27</sup> J. Langer and R. Sekerka, *Acta Metall.* **23**, 1225 (1975).
  - <sup>28</sup> G. L. Eyink, J. L. Lebowitz, and H. Spohn, *J. Stat. Phys.* **83**, 385 (1996).
  - <sup>29</sup> N. Goldenfeld, *Lectures on phase transitions and the renormalization group* (Addison-Wesley, Reading, MA, 1992).
  - <sup>30</sup> L. D. Landau and I. M. Khalatnikov, *Dokl. Akad. Nauk USSR* **96**, 469 (1954), English translation in "Collected Papers of Landau", 1965, Gordon and Breach.
  - <sup>31</sup> L. D. Landau and E. M. Lifshitz, *Mechanics* (Pergamon Press, New York, 1976).
  - <sup>32</sup> E. D. Siggia, *Phys. Rev. A* **20**, 595 (1979).
  - <sup>33</sup> D. Myers, *Surfactant Science and Technology* (John Wiley & Sons, Inc., 2005).
  - <sup>34</sup> J. Villain, *J. Phys. (Paris)* **46**, 1843 (1985).
  - <sup>35</sup> T. R. Kirkpatrick and P. G. Wolynes, *Phys. Rev. B* **36**, 8552 (1987).
  - <sup>36</sup> T. R. Kirkpatrick, D. Thirumalai, and P. G. Wolynes, *Phys. Rev. A* **40**, 1045 (1989).
  - <sup>37</sup> V. Lubchenko and P. Rabochiy, *J. Phys. Chem. B* **118**, 13744 (2014).
  - <sup>38</sup> J. Stevenson and P. G. Wolynes, *J. Phys. Chem. B* **109**, 15093 (2005).
  - <sup>39</sup> P. Rabochiy, P. G. Wolynes, and V. Lubchenko, *J. Phys. Chem. B* **117**, 15204 (2013).
  - <sup>40</sup> J. D. Stevenson, A. M. Walczak, R. W. Hall, and P. G. Wolynes, *J. Chem. Phys.* **129**, 194505 (2008).
  - <sup>41</sup> J.-P. Bouchaud and G. Biroli, *J. Chem. Phys.* **121**, 7347 (2004).
  - <sup>42</sup> V. Lubchenko and P. G. Wolynes, *J. Chem. Phys.* **121**, 2852 (2004).
  - <sup>43</sup> F. Léonforte, A. Tanguy, J. P. Wittmer, and J.-L. Barrat, *Phys. Rev. Lett.* **97**, 055501 (2006).
  - <sup>44</sup> A. Paul, S. Sengupta, and M. Rao, *J. Phys.: Condens. Matter* **26**, 015007 (2014).
  - <sup>45</sup> A. Marruzzo, W. Schirmacher, A. Fratalocchi, and G. Ruocco, *Sci. Rep.* **3**, 1407 (2013).
  - <sup>46</sup> D. Bevzenko and V. Lubchenko, *J. Phys. Chem. B* **113**, 16337 (2009).
  - <sup>47</sup> D. Bevzenko and V. Lubchenko, *J. Chem. Phys.* **141**, 174502 (2014).